

Can Monetary Policy Shocks Explain Unspanned Volatility?

Raul Riva *

Northwestern University

First Version: March, 2024

Preliminary and Incomplete - Do Not Circulate

Abstract

Affine term structure models generate sharp predictions about the time series evolution of bond yields. In special, they tie the quadratic variation of yields to the cross-section of average yields. I derive these conditions in a flexible jump-diffusion setting and use jump-robust estimators to formally test these restrictions. My approach is more general than previous techniques because it does not constrain the dynamics of underlying factors under the physical measure. I also show that two thirds of all unspanned volatility can be captured by a single factor. I investigate if this factor is related to monetary policy surprises. I find that only forward-guidance-type shocks fuel unspanned volatility, although such surprises can explain less than 10% of the unspanned volatility factor.

Keywords: Affine models, unspanned volatility, monetary policy, bipower variation, quadratic variation.

*I'd like to thank Torben Andersen, Caio Almeida, Bob Korajczyk, Viktor Todorov for helpful comments and support.
<https://rgriva.github.io/>

1 Introduction

The so-called affine term structure models are prevalent in applied research. They are flexible and can generate rich dynamics for bond yields. Additionally, the prices of different securities in such models are arbitrage-free by construction, which has great theoretical appeal. They do generate, however, very sharp restrictions on how bond prices - and yields - should behave over time. As [Duffee \(2002\)](#) points out, there is tension between fitting the cross-section of yields at a given point in time and matching the time-series dynamics of bond prices.

One typical implication of such models is that, as long as we trade more yields than underlying risk factors, all the movement of relevant state variables should be revealed (or “spanned”) by the cross-section of yields. When underlying risk factors evolve as a Markovian process, this property implies that, for example, no state variable other than the yield curve itself should help forecasting future yields and bond returns. This is a restriction on the conditional first moment of yields. It has attracted attention from the empirical literature since it’s a testable implication of such models (see [Cochrane and Piazzesi \(2005\)](#); [Ludvigson and Ng \(2009\)](#); [Cooper and Priestley \(2009\)](#); [Joslin et al. \(2014\)](#); [Cieslak and Povala \(2015\)](#); [Bauer and Hamilton \(2018\)](#); [Bianchi et al. \(2021\)](#); [Freire and Riva \(2023\)](#)).

The implications are not constrained to the conditional first moment, however. In fact, the spanning property holds path-by-path, consequently tying together both the distribution of yields and the distribution of underlying factors. Hence, from a theoretical point of view, it is natural to study the implication for second moments as well - the variances and covariances of yields. From the applied perspective, one should also be worried about how yield variances and covariances evolve since that is key for hedging fixed income portfolios.

In this paper, I derive implications for how the quadratic variation process of linear combinations of yields should behave over time if the underlying model is indeed affine. These conditions are generalizations of the ones presented by [Andersen and Benzoni \(2010\)](#). Such conditions will constrain the projection of the quadratic variation process of yields into the cross-section of average yields, generating testable implications. More specifically, in an affine jump-diffusion setting, the diffusive part of the quadratic variation process of *any* linear combination of yields must be perfectly described, or spanned, by the cross-section of average yields.

Testing such conditions when underlying factors evolve as a pure diffusion is straightforward since the realized variance of yields can approximate the quadratic variation process arbitrarily well.¹ When we allow for jumps, such tight connection breaks since the variation that is due to jumps does not need to be connected to the cross-section of bond prices anymore. [Andersen and Benzoni \(2010\)](#) design a testing procedure that bypasses this issue. But they have to constrain the dynamics of the underlying factors both under the physical and the risk-neutral measures. Additionally, they need to assume a certain martingale-like condition that might not always be satisfied.

The approach I use relies on jump-robust estimators for the diffusive part of the quadratic variation process. These estimators were introduced in [Barndorff-Nielsen and Shephard \(2004\)](#). Although perhaps less efficient than the approach used by [Andersen and Benzoni \(2010\)](#), my empirical implementation will not constrain the dynamics of underlying factors under the physical measure. Additionally, I will not have to take a stance on the empirical importance of the drift in yields at horizons like a day or a month.

¹See [Aït-Sahalia and Jacod \(2014\)](#) for a textbook treatment of theory of realized measures in the context of financial econometrics.

I use a daily dataset of zero-coupon yields constructed by [Liu and Wu \(2021\)](#) to test the implications I derive. I focus on three specific linear combinations of yields based on a Nelson-Siegel representation of the yield curve. This representation is an empirically disciplined analogue of decomposition the yield curve into level, slope and curvature factors. I find that the condition implied by affine term structure models for the volatility of yields fail across the entire yield curve. Namely, the cross-section of average yields cannot explain the volatility we measure non-parametrically on the data.

I further document that the volatility that cannot be explained by the cross-section of yields, which I call “unspanned volatility”, has a strong 1-factor structure. Such factor spikes during recessions and during moments of financial turmoil, such as the great inflation from the 1970s, the Black Monday in 1987, the first round of Quantitative Easing by the Federal Reserve in 2009, and Operation Twist in 2011. This single factor can explain two thirds of all volatility the cross-section of average yields cannot for.

As a first step into understanding the underlying causes of unspanned volatility, I test whether monetary policy surprises can account for such excess variation. And, importantly, what kind of monetary policy instrument explains unspanned volatility. I use time series of monetary policy surprises identified by [Swanson \(2021\)](#) to show that 1) overall volatility does increase when there monetary policy surprises, although the fraction of overall volatility that is due to jumps stays constant over time; 2) it’s only forward-guidance-type shocks that fuel unspanned volatility; 3) quantitatively, less than 10% of unspanned volatility can be explained by monetary policy surprises.

The paper is organized as follows. Section 2 introduces the main mathematical setup and derives implications from it. Section 3 briefly describes the two datasets I use. Section 5 tests introduces jump-robust estimators and tests the implications derived in Section 2. Section 6 quantifies the fraction of total variation that is due to jumps. Section 7 studies how much of unspanned volatility monetary policy can account for. Section 8.

2 Implications from Affine Term Structure Models

In this section, we derive implications for the volatilities of yields and, more generally, for any linear combination of yields in the affine term structure setting. Later, we will interpret the Nelson-Siegel factors as a particular linear combination of yields and all results will apply. We first concentrate on the pure diffusion case, and then we show how to extend the implications when there are jumps.

2.1 Initial Setup

Assume that X_t is an N -dimensional Ito Process with dynamics under the risk-neutral measure given by:

$$dX_t = K(\Theta - X_t) dt + \Sigma \sqrt{S_t} dW_t^Q \tag{1}$$

where dW_t^Q is an N -dimensional Brownian motion under the risk-neutral measure, K and Σ are constant $N \times N$ matrices. S_t is a diagonal matrix such that:

$$S_{t,[ii]} = s_{0,i} + s'_{1,i} X_t \tag{2}$$

We assume that S_t is positive definite with probability one.² We let the instantaneous rate be denoted by r_t and evolve according to

$$r_t = \delta_0 + \delta_1' X_t \quad (3)$$

Under these conditions, the price of a zero-coupon bond with maturity τ and its respective yield to maturity are given by

$$\log P_t^{(\tau)} = -a(\tau) - b(\tau)' X_t \quad (4)$$

$$y_t^{(\tau)} \equiv -\frac{\log P_t^{(\tau)}}{\tau} = \frac{a(\tau)}{\tau} + \frac{b(\tau)'}{\tau} X_t \quad (5)$$

where $a(\tau)$ and $b(\tau)$ are smooth functions of τ that solve a certain system of differential equations, with $a(0) = 0$ and $b(0) = 0$.³ If we stack $J \geq N$ yields with maturities ordered as in (τ_1, \dots, τ_J) into Y_t , we can effectively write

$$Y_t = A + B X_t \quad (6)$$

where A and B are functions of the parameters and the stacked maturities. A is a $J \times 1$ vector while B is a $J \times N$ matrix. As long as we can invert $B'B$, we can write

$$X_t = (B'B)^{-1} B'(Y_t - A) = \tilde{A} + \tilde{B} Y_t \quad (7)$$

This is a spanning requirement. As long as we trade more yields than underlying factors, they should reveal all information in the factors themselves. This condition should hold for each realization of yields and factors, or “path-by-path” in the language of continuous-time models.

Equation (7) is key for the results ahead. It implies that knowledge of yields is enough to characterize movements from the underlying factors - a sharp restriction on how data should behave. For instance, it implies that the conditional expectation of yields from $t + h$, given all information up to time t , should depend only on the yield curve from t . This implication regarding the *first* conditional moment has been tested in previous literature (see Ludvigson and Ng (2009); Cooper and Priestley (2009); Joslin et al. (2014); Cieslak and Povala (2015)) and more recently in Bauer and Hamilton (2018) and Freire and Riva (2023). In the current paper, I focus on implications about the *second* moment of yields.

2.2 The Quadratic Variation Process

The instantaneous variation of the process Y_t is given by

$$dY_t dY_t' = B \Sigma S_t \Sigma' B' dt \quad (8)$$

which is still of order dt since we are in a pure diffusion setting. Let c be a $J \times 1$ vector. Then, the instantaneous variation of the linear combination $L_t \equiv c' Y_t$ is given by:

$$(dL_t)^2 = c' (dY_t dY_t') c = (c' B \Sigma S_t \Sigma' B' c) dt \quad (9)$$

²This can be ensured by constraining the parameters of the model - a multidimensional Feller condition. See Duffie and Kan (1996) and Piazzesi (2010) for a discussion of such conditions. Here, we assume that these are satisfied.

³See Piazzesi (2010) for a review of basic results in this setting.

To simplify notation, we define $u \equiv \Sigma' B' c$. This is an $N \times 1$ vector. With this notation, we have that the instantaneous variation of Z_t can be written as

$$\begin{aligned}
(dL_t)^2 &= \sum_{n=1}^N u_n (s_{0,n} + s'_{1,n} X_t) dt \\
&= (\alpha_0 + \alpha'_1 X_t) dt \\
&= (\alpha_0 + \alpha'_1 (\tilde{A} + \tilde{B} Y_t)) dt \\
&= (\gamma_0 + \gamma'_1 Y_t) dt \\
&= \left(\gamma_0 + \sum_{j=1}^J \gamma_{1,j} \cdot y_t^{(\tau_j)} \right) dt
\end{aligned} \tag{10}$$

where γ_0 is a scalar and γ_1 is a $J \times 1$ vector. The second equality only collected terms, while the third one holds because of equation (7). For some time interval $h > 0$, we denote the increment to the quadratic variation process of L_t between t and $t + h$ by $QV_L(t, t + h)$:

$$\begin{aligned}
QV_L(t, t + h) &\equiv \int_t^{t+h} (dL_t)^2 = \int_t^{t+h} \left(\gamma_0 + \sum_{j=1}^J \gamma_{1,j} \cdot y_t^{(\tau_j)} \right) dt \\
&= \gamma_0 h + \sum_{j=1}^J \gamma_{1,j} \int_t^{t+h} y_t^{(\tau_j)} dt \\
&= \tilde{\gamma}_{0,i} + \sum_{j=1}^J \tilde{\gamma}_{1,i,j} \cdot \bar{y}^{(\tau_j)}(t, t + h)
\end{aligned} \tag{11}$$

in which we define $\bar{y}^{(\tau_j)}(t, t + h) \equiv \frac{1}{h} \int_t^{t+h} y_s^{(\tau_j)} ds$. This is a notion of average yield over the interval $[t, t + h]$. Equation (11) implies that the increment to the quadratic variation process of L_t between t and $t + h$ is a linear combination of the average yields over the same interval. Importantly, we highlight that both the left-hand side and the right-hand side are only known at time $t + h$. The equality in (11) holds path by path. The *econometric implication* is that a regression of quadratic variation increments on average yields should yield an R^2 of one, absent measurement error. Moreover, we would expect statistical evidence of the significance of many of the coefficients in that regression.⁴

2.3 Allowing for Jumps

Although the term structure literature typically works within a pure diffusion setting, there is no *a priori* reason to rule jumps out. There is evidence that macroeconomic announcements when revealing new information might cause asset prices - and not only bond prices - to jump. For instance, [Andersen et al. \(2007\)](#) document this behavior across different markets. [Piazzesi \(2005\)](#) explicitly allows for jumps induced by monetary policy. Alternatively, [Piazzesi \(2010\)](#) also points out that more extreme events such as wars and natural disasters might induce jumps. More recently, the coronavirus pandemic was a major event that induced both large yield movements around announcements and over the early months of 2020.

One of the most important aspects to explain the popularity of affine term structure models is their tractability and almost closed-form solutions. The functions $a(\cdot)$ and $b(\cdot)$ satisfy a system of ordinary differential equations

⁴[Andersen and Benzoni \(2010\)](#) derive a very similar condition for single-maturity yields. Here I generalize their result for any linear combination of yields - or portfolio of bonds.

that is relatively easy to solve for low values of N . In discrete time, the ordinary differential equations give place to simple recursions that only depend on model parameters.⁵ Allowing for jumps with general time-varying jump intensity and keeping tractability is not an easy trade-off.

Fortunately, [Duffie et al. \(2000\)](#) show that we can still have a tractable model with jumps if we assume that the jump intensity is affine in the state variables. On the one hand, this assumption still allows for interesting dynamics for the jump intensity. For instance, if X_t contains macroeconomic variables, the jump intensity can be an affine function of those. On the other hand, more general cases would require a different treatment.

To allow for jumps, assume the dynamics of X_t under the risk-neutral measure is given by:

$$dX_t = K(\Theta - X_t)dt + \Sigma\sqrt{S_t}dW_t^Q + Z_t dN_t^Q \quad (12)$$

where N_t^Q is a Poisson process with finite intensity λ_t and Z_t is a $N \times 1$ vector of jump sizes. We assume that Z_t is independent of W_t^Q and N_t . The random jump size Z_t is distributed according to some distribution ν^Q . We also let $\mathbb{E}[Z_t Z_t'] = \Omega$, which does not depend on time. We further assume that $\lambda_t = \lambda_0 + \lambda_1' X_t$ for some constant λ_0 and some vector λ_1 .

This setup still yields an affine mapping from factors to yields, so the spanning of X_t by Y_t will still hold, like in (7).⁶ The instantaneous variation of Y_t will now be given by:

$$dY_t \cdot dY_t' = B\Sigma S_t \Sigma' B' dt + B Z_t Z_t' B' dN_t^Q \quad (13)$$

In a similar fashion to the previous derivations, this implies the following for $L_t = c' Y_t$:

$$(dL_t)^2 = (u' S_t u) dt + (v' Z_t Z_t' v) dN_t^Q \quad (14)$$

where $u \equiv \Sigma' v$ and $v \equiv B' c$. The first term is similar to before, although the matrix B will be different since its rows solve a different system of ODEs for the diffusion-only case. The second term is new and comes from the presence of jumps.

The increments in quadratic variation between t and $t+h$ will now, as expected, incorporate two parts. As before, the first part is spanned by the cross-section of average yields following an argument analogous to the pure-diffusion setting. However, the realizations of the jumps cannot be spanned by the cross-section of yields. To have an expression for the increment $QV_L(t, t+h)$, notice that $N_{t+h} - N_t \geq 0$ is the number of realized jumps between t and $t+h$ and let $T_k(t, t+h)$ denote the stochastic k -th jump time between t and $t+h$. Then, $QV_L(t, t+h)$ can be written as:

$$QV_L(t, t+h) = \tilde{\gamma}_0 + \sum_{j=1}^J \tilde{\gamma}_{1,j} \cdot \bar{y}^{(\tau_j)}(t, t+h) + \sum_{k=1}^{N_{t+h} - N_t} v' Z_{T_k(t, t+h)} Z_{T_k(t, t+h)}' v \quad (15)$$

for some constants $\tilde{\gamma}_{0,i}$ and $\tilde{\gamma}_{1,j}$, $j = 1, \dots, J$. If there are no jumps between t and $t+h$, we take the last part as zero.

Without jumps, as noted, the projection of quadratic variation on the cross-section of average yields should generate a perfect fit. This is a testable implication that, unfortunately, is not satisfied when we work with the more realistic case of a jump-diffusion setting.

⁵See [Ang and Piazzesi \(2003\)](#) and [Duffie \(2013a,b\)](#) for a discrete-time treatment.

⁶Of course, the differential equations that implicitly define $a(\cdot)$ and $b(\cdot)$ will be different. The affine jump intensity is convenient because the expected number of jumps within a short interval, which appears in these differential equations, will be affine in X_t as well. See [Piazzesi \(2010\)](#) for further details.

To circumvent this issue, [Andersen and Benzoni \(2010\)](#) use the fact that the *expected* quadratic variation increment, $\mathbb{E}_t^Q [QV_L(t, t+h)]$, will be a linear combination of average yields due to the following:

$$\mathbb{E}_t^Q \left[\sum_{k=1}^{N_{t+h}-N_t} v' Z'_{T_k(t,t+h)} Z'_{T_k(t,t+h)} v \right] = \mathbb{E}_t^Q \left[\int_t^{t+h} (\lambda_0 + \lambda_1' X_s) ds \right] v' \Omega v$$

Moreover, the expected increment in quadratic variation is related to the conditional variance of yields. They are in fact equal to each other if one assumes that a certain martingale condition holds for yields. I pursue a different path and adopt a jump-robust estimator for the diffusive part of the quadratic variation process, along the lines of [Barndorff-Nielsen and Shephard \(2004\)](#). This approach won't require any other extra assumptions on this setup.

To finish this section, I highlight another related implication regarding the quadratic covariation process of different linear combinations of yields in this context. Let c and \check{c} denote $J \times 1$ vectors. We consider two linear combinations of yields: $L_t = c' Y_t$ and $\check{L}_t = \check{c}' Y_t$. The generalization of (14) brings the instantaneous covariation:

$$dL_t \cdot d\check{L}_t = (u' S_t \check{u}) dt + (v' Z_t Z_t' \check{v}) dN_t^Q$$

where $\check{u} \equiv \Sigma' \check{v}$ and $\check{v} = B' \check{c}$. We can follow the same steps that led us to (15) and we will conclude that the increment to the quadratic covariation process between L_t and \check{L}_t over the interval $[t, t+h]$ is composed by two terms analogous to the ones in (15) (obviously with different γ 's that will depend both on c and on \check{c}). The first one should be spanned by the cross-section of average yields, while the second one is due to jumps. When $c = \check{c}$, the quadratic covariation process is exactly given by (15).

3 Data

There two sources of data for the empirical implementation below. The first one is the zero-coupon nominal yield curve from [Liu and Wu \(2021\)](#). This is a daily dataset with maturities ranging from 1 to 360 months. This dataset is becoming the default source for zero-coupon yields in the empirical term structure literature. For instance, [Bianchi et al. \(2021\)](#) and [Freire and Riva \(2023\)](#) use this dataset to study the conditional mean of bond returns and yields more generally. This dataset has some advantages over other popular choices, such as the one introduced in [Fama and Bliss \(1987\)](#) and the one from [Gurkaynak et al. \(2007\)](#). The sample used in this paper ranges from January, 1973 up to December, 2022. The advantage of not using intraday data is that I can extend back the sample way longer.

In comparison to [Fama and Bliss \(1987\)](#), [Liu and Wu \(2021\)](#) provide many more maturities. That is key for us to estimate Nelson-Siegel factors since the identification of these factors relies on the fact we trade a large number of maturities. In comparison to [Gurkaynak et al. \(2007\)](#), [Liu and Wu \(2021\)](#) achieve a better fit of the shorter end of the yield curve, which is typically crucial for the pricing of different contracts.

The second dataset I rely on was developed and described in [Swanson \(2021\)](#). In similar spirit to [Kuttner \(2001\)](#) and [Gürkaynak et al. \(2005\)](#), [Swanson \(2021\)](#) considers a panel of narrow-window returns of Eurodollar and Fed Funds futures around FOMC announcements. These are considered as surprises in prices. He then extracts three principal components of this panel, and then rotate the principal components so that the first shock represents a Fed Funds rate shock, a second one represents a "forward guidance" innovation, and the third one is related to Quantitative Easing. The sample used in this paper ranges from January, 1991 up to June, 2019.

4 The Nelson-Siegel Representation

The empirical reduced-form literature on yield curve modelling and forecasting frequently deploys the so called Nelson-Siegel representation, due to [Nelson and Siegel \(1987\)](#). This approach models yields across the maturity spectrum as a linear combination of three factors:⁷

$$y_t^{(\tau)} = \beta_{t,1} + \beta_{2,t} \left(\frac{1 - e^{-\lambda\tau}}{\lambda\tau} \right) + \beta_{3,t} \left(\frac{1 - e^{-\lambda\tau}}{\lambda\tau} - e^{-\lambda\tau} \right) \quad (16)$$

Each of these factors is multiplied by a coefficient that depends on the maturity τ and on a decay parameter $\lambda > 0$. This parameter controls the shape of these coefficients as functions of τ . The coefficient that multiplies β_2 starts at one when $\tau = 0$ and decays to zero as τ increases. This decay is faster with higher values of λ . The coefficient that multiplies β_3 starts at zero when $\tau = 0$, starts increasing until it finds its maximum, and then decreases towards zero again. The maximum is reached at a maturity that depends on λ . The coefficient that multiplies β_1 is constant across maturities. Hence, the Nelson-Siegel representation is flexible enough to accommodate different shapes of the yield curve. It can generate upward-sloping, downward-sloping, and humped yield curves.⁸

These time-varying factors are empirically related to the level, slope, and curvature of the yield curve. Nonetheless, the preferred interpretation here is one related to long, short, and medium-run factors. For $\lambda > 0$, one can see that $\lim_{\tau \rightarrow \infty} y_t^{(\tau)} = \beta_{1,t}$. This motivates calling $\beta_{1,t}$ a long-term factor since it's identified as the very long end of the yield. On the other hand, all else equal, movements in $\beta_{2,t}$ are translated to larger movements at the short end of the yield curve than movements on the long end. That motivates the interpretation of $\beta_{2,t}$ as a short-run factor. Similarly, the effect of $\beta_{3,t}$ on the yield curve is minimal both at the short end and the long end. It concentrates its effect around the peak of its coefficient - an intermediate part of the yield curve. This interpretation enables us to test theories regarding the evolution of yields for different parts of the yield curve, without having to pick specific maturities. The Nelson-Siegel representation offers a straightforward decomposition of the entire yield curve with coefficients that, unlike in a PCA approach, are identified without any rotation choice and that are easy to interpret.

In principle, λ could depend on t as well. In that case, one could estimate factors and the decay parameter with non-linear least squares, for instance. However, as [Diebold and Li \(2006\)](#) stressed, a constant decay parameter is typically enough to generate a good fit and in that case we avoid numerical optimization completely. With a constant decay value, the factors $(\beta_{t,1}; \beta_{t,2}; \beta_{t,3})$ can be estimated with ordinary least squares, as outlined below. [Freire and Riva \(2023\)](#) studied different methods of estimating the decay parameter, including non-linear least squares, and showed that the observation from [Diebold and Li \(2006\)](#) is still valid almost two decades later. Whenever numerical optimization for the estimation of λ converges to a local minimum, the estimated factors were very close to the ones obtained by ordinary least squares and a constant decay parameter. The optimization didn't always converge, however. That motivates me to choose a constant decay parameter.

[Diebold and Li \(2006\)](#) used $\lambda = 0.0609$, which places the hump from the coefficient on β_3 at $\tau = 30$ months. [Freire and Riva \(2023\)](#), using a monthly panel of nominal yields, found that $\lambda = 0.0435$ would be the best constant

⁷[Svensson \(1994\)](#) extends this representation to a four-factor model. As [Diebold and Rudebusch \(2013\)](#) point out, the extension implies a model that is harder to estimate and that delivers a similar fit on the cross-section of yields. Due to its simplicity and good fit on the daily nominal yield data I use, I stick with the three-factor model. That was also the choice of [Diebold and Li \(2006\)](#); [Diebold et al. \(2006\)](#); [Hännikäinen \(2017\)](#); [Fernandes and Vieira \(2019\)](#); [Freire and Riva \(2023\)](#), among others.

⁸See [Diebold and Rudebusch \(2013\)](#) for an in-depth discussion of the properties of the Nelson-Siegel representation.

decay parameter to minimize the average squared error when fitting the cross-section of yields over their sample. But the fitting error was very similar to the one provided by the calibration from [Diebold and Li \(2006\)](#). To maintain consistency with prior literature who used the same calibration, I stick with $\lambda = 0.0609$.

4.1 Estimation

For a fixed set of maturities (τ_1, \dots, τ_J) , if we stack the corresponding zero-coupon yields in a vector Y_t , we can write the OLS estimator for the factors as

$$\begin{bmatrix} \widehat{\beta}_{1,t} \\ \widehat{\beta}_{2,t} \\ \widehat{\beta}_{3,t} \end{bmatrix} = (M'M)^{-1} M'Y_t, \quad M \equiv \begin{bmatrix} 1 & \frac{1-e^{-\lambda\tau_1}}{\lambda\tau_1} & \frac{1-e^{\lambda\tau_1}}{\lambda\tau_1} & -e^{-\lambda\tau_1} \\ 1 & \frac{1-e^{-\lambda\tau_2}}{\lambda\tau_2} & \frac{1-e^{\lambda\tau_2}}{\lambda\tau_2} & -e^{-\lambda\tau_2} \\ \vdots & \vdots & \vdots & \vdots \\ 1 & \frac{1-e^{-\lambda\tau_J}}{\lambda\tau_J} & \frac{1-e^{\lambda\tau_J}}{\lambda\tau_J} & -e^{-\lambda\tau_J} \end{bmatrix}. \quad (17)$$

Importantly, this approach implies that estimated factors are *linear combinations* of yields. In general, we write $\widehat{\beta}_{i,t} = c'_i Y_t$, where c'_i is the i -th row of $(M'M)^{-1} M'$. Since M does not depend on t , these linear combinations are not time-varying. Therefore, the implications we derived for the quadratic variation of linear combinations of yields in Section 2 will readily apply. Since we observe yields at the daily frequency, we have daily factor estimates as well.

One limitation of this approach is the necessity of a balanced panel of yields. If we change the set of available maturities, we would change matrix M and change how the factors are identified. A larger value of J implies that we use more data to estimate factors, but it will limit us in the time-series dimension since longer yields started being traded only more recently. We take $J = 120$, which implies that we use information from the 1-month yield up to the 10-year one. We start the sample in January, 1973 since the 10-year bond started being traded during the last months of 1972. The sample ends in December, 2022 which is the last available date on the daily dataset from [Liu and Wu \(2021\)](#) as the time of writing.⁹ This sample covers different scenarios both for monetary policy and business cycle. For instance, it includes the monetary tightening during the late 1970s and 1980s, the dot-com bubble burst in early 2000, the global financial crisis from 2008, the period of unconventional monetary policy, and part of the aftermath from the coronavirus pandemic.

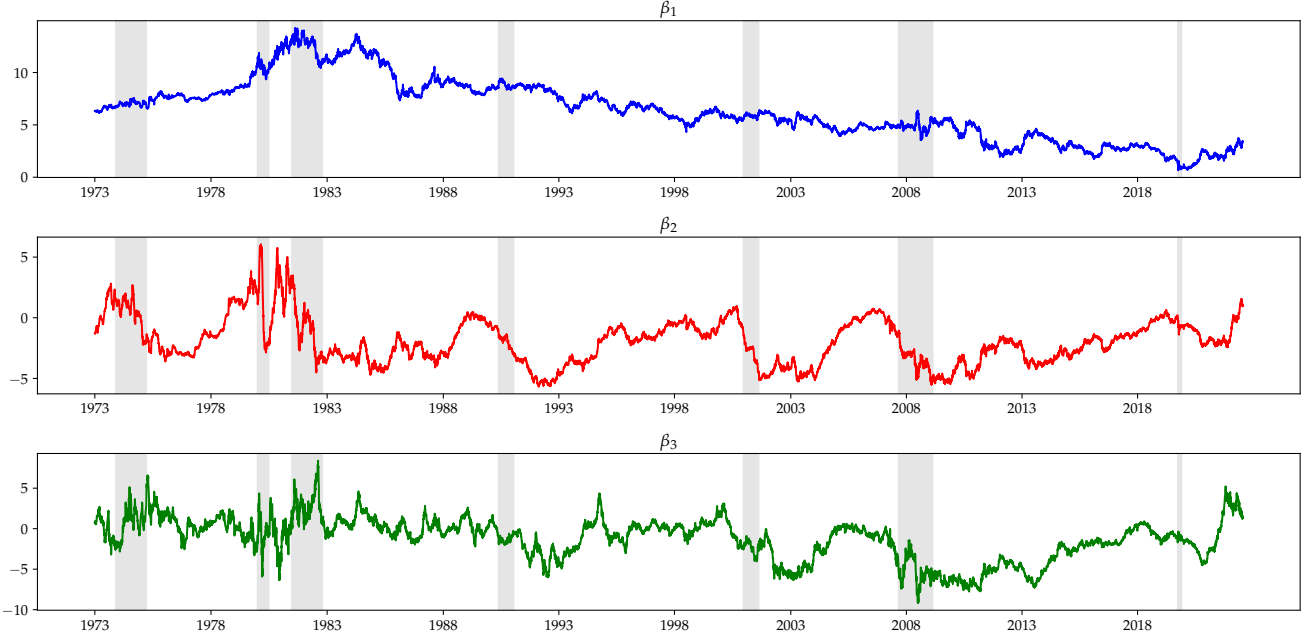
Figure 1 displays the daily estimates of factors, using daily yields from [Liu and Wu \(2021\)](#). All three factors are persistent time series, displaying trends at the business-cycle length. The long-run factor shows a steady decline since the early 1980s, following the overall decline of the US yield curve level.¹⁰ Both the short-run and the middle-run sector oscillate around negative means, which is consistent with a concave upward-sloping yield curve.

The quality of the cross-sectional fit of the Nelson-Siegel representation is stressed by [Diebold and Li \(2006\)](#) and [Gurkaynak et al. \(2007\)](#) on earlier data. [Freire and Riva \(2023\)](#) also find low fitting errors using monthly data on a sample similar to the one used in this paper. Figure A.1 in Appendix A reports the daily RMSE when fitting the cross-section of yields, which is given by $\widehat{\sigma}_t \equiv \sqrt{\frac{1}{J} \cdot \sum_{j=1}^J \left(y_t^{(\tau_j)} - \widehat{y}_t^{(\tau_j)} \right)^2}$. I report the series in basis points. The average daily RMSE is around 6 basis points, but it's constantly below 5bps. When we take into consideration that

⁹See Cynthia Wu's website: <https://sites.google.com/view/jingcynthiawu/>

¹⁰See [Bauer and Rudebusch \(2020\)](#) for a treatment of this decline and further implications for yield curve models.

Figure 1: Daily time-series of Nelson-Siegel factors estimated using the zero-coupon data from Liu and Wu (2021). The sample ranges from 1973 to 2022. All maturities from 1 to 120 months are used. Gray bars denote NBER recessions.



these are annualized yields, we conclude that the Nelson-Siegel representation achieves an impressive fit on the dataset from Liu and Wu (2021).

4.2 Realized Covariances and Bipower Covariation

We now turn to the estimation of the realized covariances of the Nelson-Siegel factors, as well as the bipower covariation measures. To ease notation, I drop the “hat” sign from the β ’s although these variables refer to the estimated factors from Figure 1. From the daily time series of factor estimates, I estimate the realized covariance measures within each month. Formally, let’s define the realized covariance between factor i and factor j during month t as:

$$RCov_{i,j}(t) \equiv 12 \cdot \sum_{d=1}^{D_t} \left(\beta_{i,t+d/D_t} - \beta_{i,t+(d-1)/D_t} \right) \cdot \left(\beta_{j,t+d/D_t} - \beta_{j,t+(d-1)/D_t} \right) \quad (18)$$

where D_t denotes the number of trading days within month t . We multiply the sum by 12 to have an annualized amount. When $i = j$, we have the usual realized variance measure. In that case, we call the square root of (18) the realized volatility of factor i . As D_t increases, $RCov_{i,j}(t)$ approximates the quadratic covariation over month t arbitrarily well.¹¹

Similarly, I follow Barndorff-Nielsen and Shephard (2004) and define the realized bipower variation of factor i as:

$$BPV_i(t) \equiv 12 \cdot \frac{\pi}{2} \cdot \sum_{d=2}^{D_t} \left| \beta_{i,t+d/D_t} - \beta_{i,t+(d-1)/D_t} \right| \cdot \left| \beta_{i,t+(d-1)/D_t} - \beta_{i,t+(d-2)/D_t} \right| \quad (19)$$

As shown in Barndorff-Nielsen and Shephard (2004), as D_t increases, the random variable defined in equation

¹¹See Andersen and Benzoni (2008) for a review of these techniques and Ait-Sahalia and Jacod (2014) for a full textbook treatment.

(19) approximates the part of the quadratic variation process that comes from the diffusive part from (12). It won't be disturbed by the jumps. Alternatively, when we work in a pure diffusion setting, both (18) and (19) estimate the same quantity.¹² Accordingly, the difference $RCov_{i,i} - BPV_i$ converges in probability to the part of the quadratic variation process that depends on jumps. In our context, that is the last term in equation (15).

The intuition why BPV_i is able to estimate only the diffusive part comes from the fact that, over short intervals, the presence of many jumps become increasingly unlikely. As the sampling becomes more frequent, jumps start being confined to a single interval of decreasing length $1/D_t$. When there are no jumps, the quadratic variation process has increments of order dt . As dt decreases, intuitively, at least one of the terms in the typical product inside the summation in (19) will be small enough to guard the estimator against jumps.

Notice that we have defined only the realized bipower variation for a single factor. But, as also demonstrated by Barndorff-Nielsen and Shephard (2004), we can extend that definition and define the realized bipower covariation. That is done using a polarization identity. Denoting by $BPV_{i+j}(t)$ the bipower variation of the time series composed by sum of $\beta_{i,t}$ and $\beta_{j,t}$, the realized bipower covariation between factors i and j over month t is given by:

$$BPCov_{i,j}(t) \equiv \frac{1}{2} (BPV_{i+j}(t) - BPV_i(t) - BPV_j(t)) \quad (20)$$

This random variable estimates the diffusive part of the quadratic covariation process between factors i and j . Once again, when we are in the diffusion-only setting, $RCov_{i,j}$ and $BPCov_{i,j}$ estimate the same quantity. And, in general, when $i = j$ we have that $BPCov_{i,i}(t) = BPV_i(t)$. Finally, we also note that both $RCov_{i,j}$ and $BPCov_{i,j}$ can be negative when $i \neq j$.

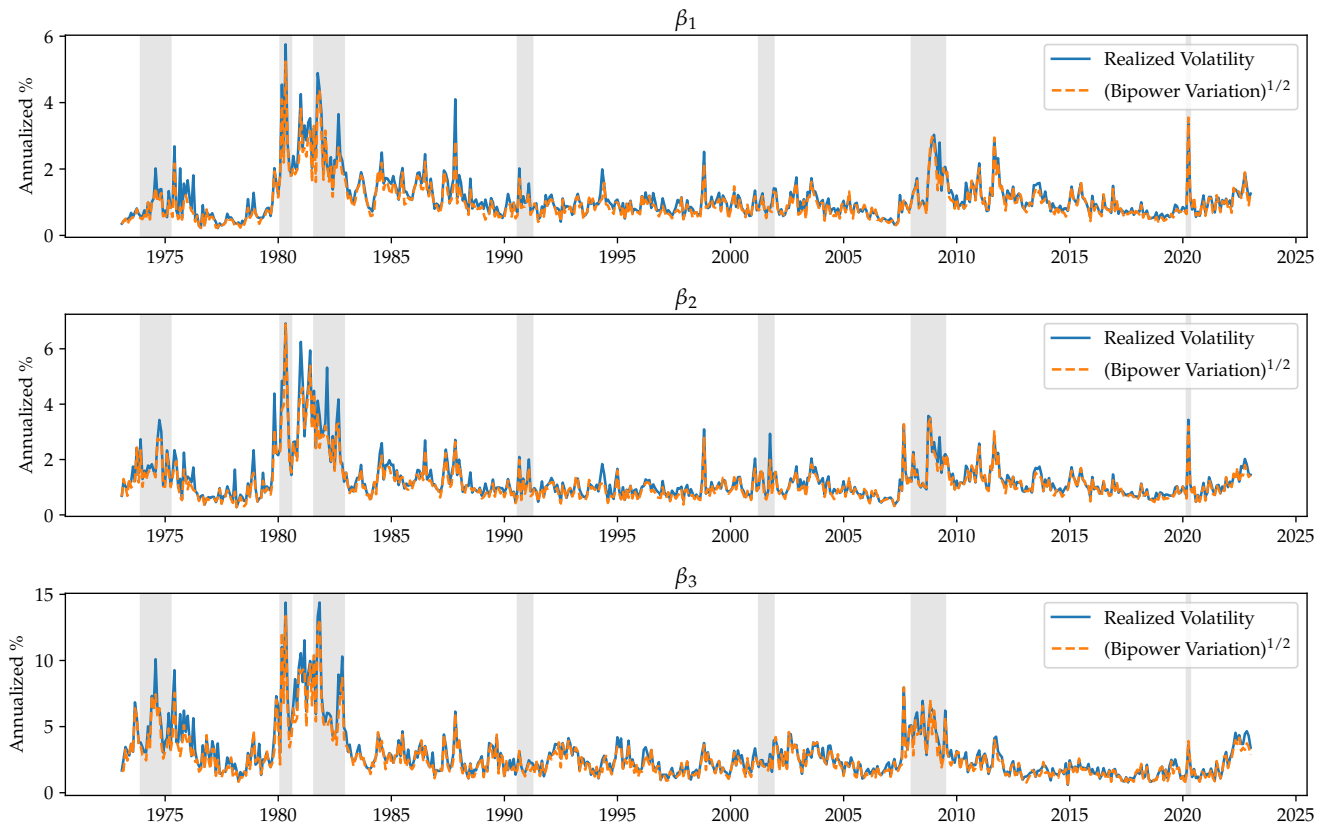
Figure 2 displays the monthly realized volatility (the square root of realized variance) of each factor as a blue solid line, and the square root of BP_i as a dashed orange line. For all three factors, they are very close. The difference between them can be taken as a consistent estimator of the part of the quadratic variation process that is due to the jumps. The periods of higher volatility are the 1970s and the 1980s. That is due to very active monetary policy during in special after Paul Volcker became the chairman of the Federal Reserve in 1979. Volatility also spikes up during periods of crises such as the period just after 2008 and in early 2020. In Appendix A, Figure A.2 displays a similar plot focusing on the the realized covariation between factors and the associated bipower covariation. In that we see that these time-series are very close to zero most of time, with the exception of the early mid 1970s and early 1980s.

Table 1 displays summary statistics for the realized covariances and realized bipower covariation measures. The total sample is 600 observations since these measures are at the monthly frequency, starting in January, 1973 and ending in December, 2022. We see that variation measures related to the medium-run factor β_3 are typically higher than the other ones. That can also be seen from Figure A.2 since the scales are different. That factor is the hardest one to identify (see Diebold and Rudebusch (2013)). Hence, the variation measures might contain more noise in that case. The variation measures are skewed, with mean values just above the respective 75% percentile, both for realized variance and realized bipower variation measures.

In order to validate these measures, we now explore two salient periods and compare movements of the entire yield curve with the respective variation measures shown in Figure 2. The first period is related to start of Paul Volcker's chairmanship at the Federal Reserve. His tenure ranged from August, 1979 up to August, 1987. The first

¹²Simulation evidence from Barndorff-Nielsen and Shephard (2004) suggests that the realized variance is a more efficient estimator in the case of a pure diffusion, nonetheless.

Figure 2: Realized volatility (solid blue line) and the square root of realized bipower variation (dashed orange) for each of the Nelson-Siegel factors. All measures are annualized, but computed at the monthly frequency.



years of his tenure represented a period of unprecedented monetary tightening to combat the high inflation from the 1970s.¹³ The first panel in Figure 3 displays end-of-month yield curves starting in August, 1979 and ending in December, 1983. Colors evolve following the timeline, from darker to lighter shades.

The yield curve from December, 1979 had a similar shape although a very different level than the one from August of the same year. In July, 1980 it had a different shape, now with an upward-sloping profile. Between December, 1980 and July, 1981 there was a slight change in slope although the level was similar - even though the level was much higher than a few months before. In 1982 the yield curve was already sloping upwards again and it became gradually steeper until December, 1983. All these movements regarding the level, the slope and the humps in these curves are translated to high measures of yield variation, as seen in Figure 2, regardless of our estimator choice.

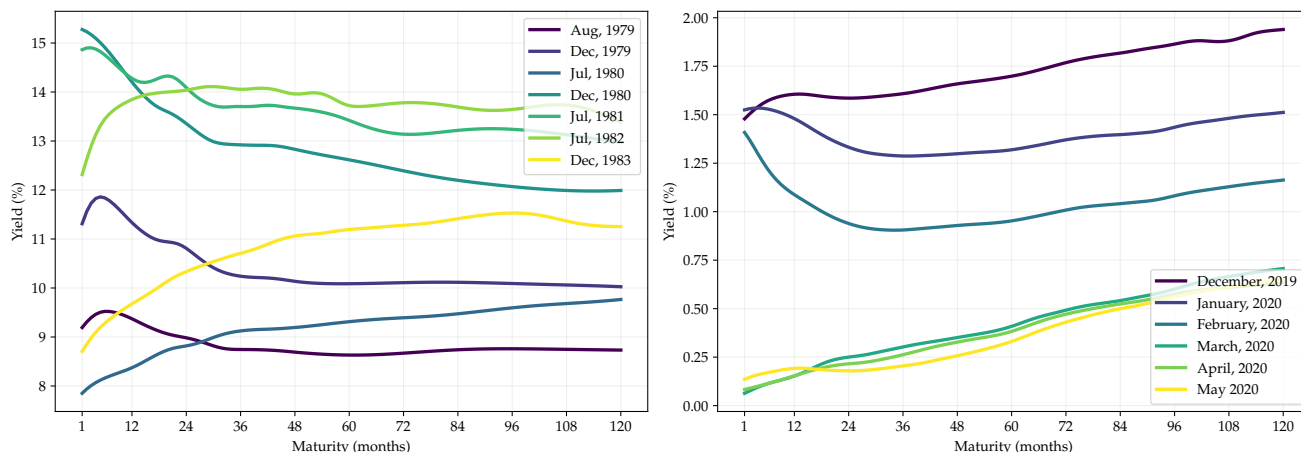
The second panel in Figure 3 analyzes yield curve movements during the early months of 2020 when the coronavirus pandemic hit the American economy. At the end of 2019, the yield curve was upward sloping. During the next two following months, it became downward sloping - a change also followed by a decrease in the level of the entire curve. At the end of March, it was almost a linear function of the maturity once again, with a positive slope. However, at an even lower level. These movements are translated to high readings of realized volatility for March, 2020 in Figure 2. That is stronger for β_1 and β_2 , a consequence of stark changes in both level and slope.

¹³See [Blinder \(2022\)](#) for a detailed account.

Table 1: Summary statistics for annualized realized covariation and realized bipower covariation measures. The sample goes from 1973 to 2022.

	Sample Size	Mean	Std. Dev.	5% pct.	25% pct.	50% pct.	75% pct.	95% pct.
$RCov_{11}$	600	1.69	2.80	0.24	0.51	0.92	1.66	5.83
$RCov_{22}$	600	2.30	4.29	0.32	0.67	1.06	2.02	8.07
$RCov_{33}$	600	11.76	21.26	1.26	2.94	5.33	11.35	41.19
$RCov_{21}$	600	-1.24	1.93	-3.95	-1.41	-0.72	-0.42	-0.08
$RCov_{31}$	600	-1.56	4.92	-7.68	-1.43	-0.43	0.20	1.16
$RCov_{32}$	600	0.30	3.32	-2.52	-0.68	-0.04	0.70	5.52
BPV_1	600	1.39	2.30	0.19	0.42	0.76	1.33	4.62
BPV_2	600	1.90	3.46	0.26	0.54	0.93	1.76	7.33
BPV_3	600	9.75	18.06	1.10	2.42	4.56	9.30	34.37
$BPCov_{21}$	600	-1.03	1.66	-3.23	-1.23	-0.64	-0.33	-0.06
$BPCov_{31}$	600	-1.31	4.14	-5.98	-1.35	-0.43	0.15	1.04
$BPCov_{32}$	600	0.25	3.48	-2.49	-0.64	-0.03	0.64	3.61

Figure 3: End-of-month yield curves at different salient moments: great inflation and early Volcker years (left) and late 2019/early 2020 close to the coronavirus pandemic (right). All yields are annualized.



As a final check, Figure A.4 in Appendix A reports a comparison between the time-series of realized volatility for each factor using either a balanced panel of yields (as in Figure 2) or an unbalanced one, which uses all the available maturities from Liu and Wu (2021). These measures track each other. The correlation between them is higher than 0.9 in all cases and higher than 0.97 for β_1 and β_2 . Although using an unbalanced panel gives us a longer time series, the linear combinations that define the factors are not constant over time. That would invalidate some of the implications derived in Section 2. The choice of a balanced panel makes the previous computations precise and is immaterial for the empirical results.

5 Unspanned Volatility Everywhere

This section tests the implications from Section 2. I highlight once more that, in this context, the Nelson-Siegel factors should be understood as linear combinations of yields. In a pure diffusion setting, the quadratic variation increment during month t should be spanned by the cross-section of average yields, which can be approximated by the realized covariances. That is not true anymore in a jump-diffusion setting. However, the bipower variation (and covariation) measures are robust to jumps and estimate *only* the diffusive part of the quadratic variation process.

My approach is different than the one taken by Andersen and Benzoni (2010) because they need to assume extra conditions on yields to tie the expected quadratic variation to the conditional variance of yields. Those conditions are less likely to be satisfied at the monthly frequency used in this paper. More importantly, they need to assume that the dynamics of X_t is affine under *both* the risk-neutral and the physical measure. My approach does not rely on any assumptions related to the P measure.¹⁴

Additionally, instead of casting the analyses at the single maturity level, I test the implications from affine term structure models over the entire yield curve, using the Nelson-Siegel representation as a disciplined way of decomposing the yield curve movements through the movement of the factors. Freire and Riva (2023) analyze the conditional mean of these factors and show that state variables such as macroeconomic indicators can only help forecasting β_2 , providing no gain for the other factors. There phenomena creates “unspanned” risk premium. Hence, it’s natural to ask here whether we find unspanned volatility through all factors.

5.1 Linear Projections

The derivations from Section 2 suggest two different regression specifications. Let’s denote by \bar{Y}_t the $J \times 1$ vector of average yields over month t . Its j -th element is given by $\bar{y}^{(\tau_j)}(t, t+h) \equiv \frac{1}{h} \int_t^{t+h} y_s^{(\tau_j)} ds$. Then, it’s natural to study the following regressions:

$$RCov_{i,j}(t) = \alpha_{i,j} + \gamma'_{i,j} \bar{Y}_t + \epsilon_{i,j}(t), \quad i, j = 1, 2, 3 \quad (21)$$

$$BPCov_{i,j}(t) = \delta_{i,j} + \theta'_{i,j} \bar{Y}_t + \eta_{i,j}(t), \quad i, j = 1, 2, 3 \quad (22)$$

We could approximate each element of \bar{Y}_t by the average yield within a month. However, since Litterman and Scheinkman (1991), we know that the cross-section of yields have a factor structure of low dimension. Hence, we use the average Nelson-Siegel factors within month t as the variables on the right-hand side of regressions (21) and (22). As a robustness check, I will also report results using principal components of yields.

Absent measurement error, the fit in both cases should be perfect under the pure-diffusion setting and it should also be perfect for (22) in the case of a jump-diffusion underlying process X_t . A perfect fit is identified by $R^2 = 1$ in these regressions. We now test these implications.

Table 2 reports coefficient estimates and associated R^2 values for the specification in (21). The three first

¹⁴Models that fall into the “essentially affine” class introduced by Duffee (2002) have the property of being affine both under P and Q . Although this class is prevalent, there are exceptions. For example, Duarte (2004) uses a richer parametrization for the price of risk. But his model is not affine under P anymore. My approach would handle both cases.

columns use the realized variances as dependent variables while the three last ones study the realized covariances. Standard errors are based on a HAC-adjusted covariance matrix using the estimator from [Newey and West \(1987\)](#).

Panel A uses the full sample, ranging from 1973 up to 2022. These are exactly 600 monthly observations. In fact, we do find that the coefficients on the average value of factors are often significant, in special for the average value for β_1 . One exception is $RCov_{32}$, for which we find no significant coefficients. The most salient fact, nonetheless, are the very low R^2 . These values are higher than the numbers reported in [Andersen and Benzoni \(2010\)](#) but their sample only starts in the 1990s. In any case, these R^2 values are far from 1.

As described in detail by [Blinder \(2022\)](#) and [Bernanke \(2023\)](#), Volcker's tenure at the Federal Reserve, which corresponds to the initial period of the sample at hand and also to the period of more extreme readings of realized variance measures, was exceptional in a number of ways. Inflation levels were at two digits and there was a sharp tightening of monetary policy. There was also an ongoing discussion of how to conduct monetary policy itself: either via monetary aggregates or via interest rate setting.¹⁵ Additionally, central bank communication was done in a way that can probably be described as less transparent than nowadays.¹⁶ This exceptionality motivates dividing our full sample in two subsamples. The first subsample starts in 1973 and ends in August, 1987 - when Volcker left the Federal Reserve. The second subsample starts in September, 1987 and ends in December, 2022.

Panels B and C in [Table 2](#) repeat the analysis from Panel A but for the other two subsamples. Panel B reports coefficient estimates that are typically significant both for the average value of β_1 and the average value of β_2 . The coefficient on the average value of β_3 is not significant in general. Once more, we found no significant coefficients from $RCov_{32}$. The R^2 values are higher than in Panel A, but they are still far from 1. Panel C reports even starker results. In that case, we find essentially no significant coefficients and R^2 values that are never higher than 0.11, once again far from 1. The lack of significance of these coefficients and even lower values for R^2 suggest that the cross-section of yields became even worse at spanning the volatility measures it should, in theory, span when we focus on more recent samples.

One explanation for these low values of R^2 could be the presence of jumps. As shown in [\(15\)](#) this would break the spanning condition and could generate values of R^2 that are lower than 1. However, the realized bipower variation (and covariation) measures are robust to jumps and estimate only the part that should be spanned by the cross-section of yields. We now study specifications as in [\(22\)](#).

[Table 3](#) repeats the analysis present in [Table 2](#) but with the realized bipower covariation measures as dependent variables. We see similar qualitative and quantitative patterns. For the full sample, most of the coefficients are significant but R^2 values are never higher than 0.31, which is far from the ideal value of 1. The subsample that ends in August, 1987 generates similar results. The R^2 values are higher in for all six regressions but they are once more far from 1. Finally, the last panel from [Table 3](#) reports results for the second subsample. Results are stark again. We find no significant coefficients and the highest R^2 value is 0.13.

In summary, the evidence so far leads us to conclude that, even when we account for the presence of jumps, the cross-section of yields cannot span the volatility measures it should, following the implications of standard affine term structure models. There is also suggestive evidence, judging by the lack of significance of coefficients and very low R^2 values, that the problem of *unspanned* volatility became, if anything, starker over time. To the best

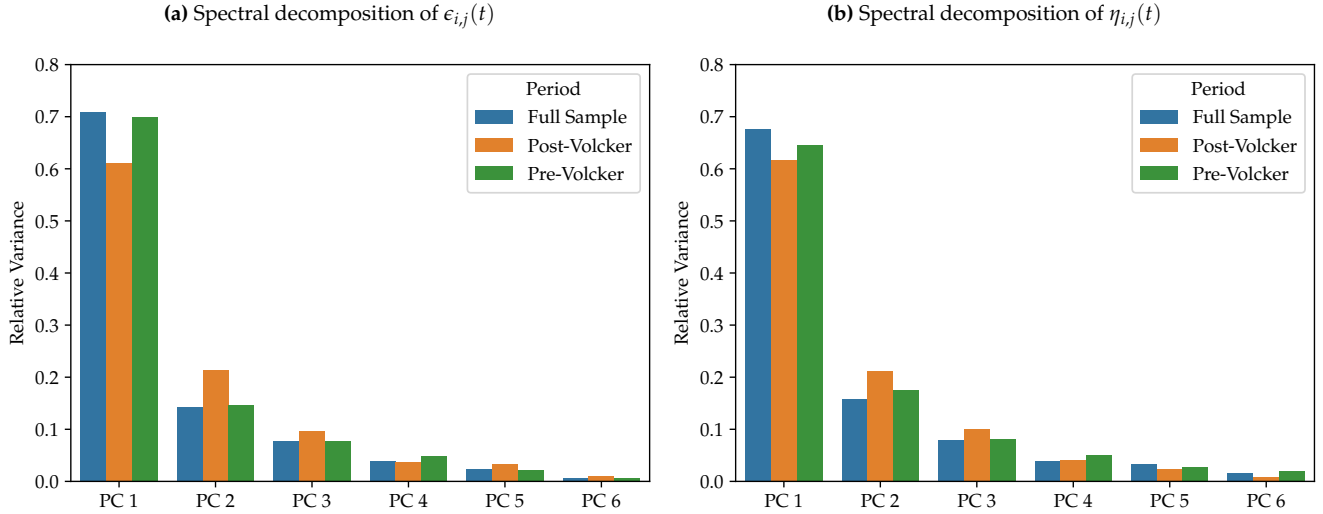
¹⁵See [Bernanke \(2023\)](#) for an account of these methodological discussions.

¹⁶For instance, the Federal Open Market Committee only started announcing Fed Funds targets in 1995 and systematic press conferences started during Bernanke's tenure.

Table 2: Coefficient estimates from (21). Variables are always standardized before running the regression. Standard errors are computed using the HAC estimator from Newey and West (1987). Stars denote significance at 10%, 5%, and 1%, respectively. Different panels refer to different subsamples.

Panel A: Full Sample (January, 1973 - December, 2022)						
	$RCov_{11}$	$RCov_{22}$	$RCov_{33}$	$RCov_{21}$	$RCov_{31}$	$RCov_{32}$
Average β_1	0.433*** (0.136)	0.714*** (0.213)	3.361*** (1.041)	-0.190** (0.079)	-0.671*** (0.233)	0.173 (0.118)
Average β_2	0.398* (0.225)	1.106*** (0.392)	4.257** (1.684)	-0.186 (0.136)	-0.805** (0.340)	0.129 (0.154)
Average β_3	-0.267* (0.145)	-0.631** (0.245)	-1.587 (1.116)	0.210** (0.093)	0.280 (0.221)	-0.043 (0.115)
N	600	600	600	600	600	600
R^2	0.20	0.32	0.27	0.09	0.20	0.02
Panel B: High Inflation and Volcker's Tenure (January, 1973 - August, 1987)						
	$RCov_{11}$	$RCov_{22}$	$RCov_{33}$	$RCov_{21}$	$RCov_{31}$	$RCov_{32}$
Average β_1	1.061*** (0.208)	1.440*** (0.287)	5.543*** (1.826)	-0.525*** (0.131)	-1.254*** (0.461)	0.232 (0.341)
Average β_2	0.765*** (0.213)	1.815*** (0.349)	8.527*** (1.792)	-0.396*** (0.143)	-1.544*** (0.458)	0.290 (0.290)
Average β_3	0.201 (0.269)	-0.106 (0.386)	3.848* (2.106)	-0.043 (0.189)	-0.974* (0.559)	0.468 (0.423)
N	176	176	176	176	176	176
R^2	0.39	0.49	0.39	0.22	0.30	0.04
Panel C: Post-Volcker Sample (September, 1987 - December, 2022)						
	$RCov_{11}$	$RCov_{22}$	$RCov_{33}$	$RCov_{21}$	$RCov_{31}$	$RCov_{32}$
Average β_1	0.010 (0.051)	0.002 (0.055)	0.409 (0.367)	0.048 (0.043)	0.006 (0.059)	-0.013 (0.058)
Average β_2	-0.087 (0.091)	-0.043 (0.088)	-0.545 (0.603)	0.103 (0.071)	-0.065 (0.122)	0.076 (0.130)
Average β_3	-0.092 (0.094)	-0.153 (0.095)	-0.232 (0.641)	0.103 (0.077)	0.174 (0.114)	-0.149* (0.088)
N	424	424	424	424	424	424
R^2	0.06	0.07	0.05	0.11	0.04	0.03

Figure 4: Spectral decomposition of the panels of residuals from (21) and (22). Before applying the diagonalization, the series are demeaned and standardized. See Table B.1 for the definitions of the subsamples.



of my knowledge, this is the first study to document this apparent asymmetry between these two subsamples.

5.2 Isn't it just noisy measurements?

One possible concern is that the daily sampling of yields is too coarse and does not allow for precise measurement of realized variances and realized bipower variation measures. That would generate noisy measurements, which would lower the R^2 in the regressions above. In principle, these measures will always contain some noise since they only match the realization of the respective population moments when D_t diverges to infinity. In this section, I provide evidence that the low R^2 are *not* driven solely by noise.¹⁷

To analyze this issue, I focus on studying the regression residuals from (21) and (22). For each time t , there are six residuals - one from each regression. If the low R^2 values are only due to noisy volatility measurements, then the time series of residuals should have no factor structure. I consider the spectral decomposition of the covariance matrix of these residuals, after scaling them to have have same standard deviation.

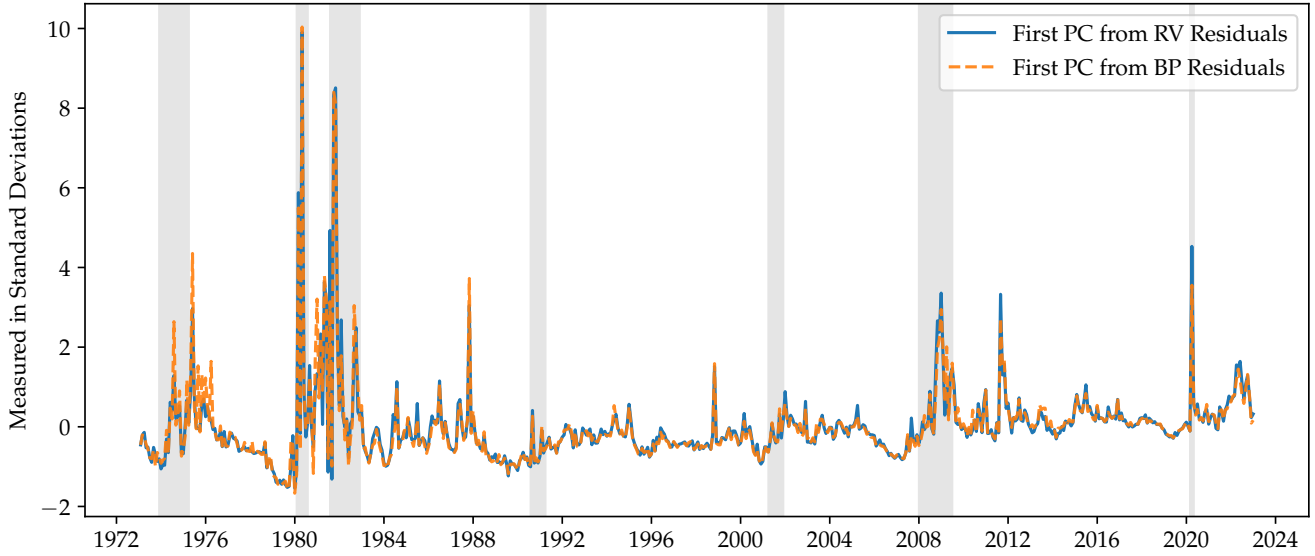
Figure 4 reports the fraction of total variance explained by each of the principal components from the panel constructed from $\epsilon_{i,t}(t)$ (left) and the one constructed from $\eta_{i,j}(t)$ (right). The different bars report results for different subsamples. In any case, I find evidence of a dominant factor driving *unspanned* variances (and covariances) - no matter whether we account for jumps or not. Using the full sample, the first principal component explains around 70% of the total variance when we consider the residuals from (21). The same pattern arises when we use the residuals from (22), for which the first principal component explains just short of 70% of the total variance of the panel of residuals. Although the realized covariances and bipower covariation measures are undoubtedly noisy to some extent, it's hard to explain the low R^2 values from Tables 2 and 3 in light of the evidence from Figure 4. Pure noise wouldn't have such a factor structure.

¹⁷Notice that [Barndorff-Nielsen and Shephard \(2006\)](#) develop a Central Limit Theorem for the measures used in this paper. Hence, we could in principle create confidence bands for the realized covariances and bipower covariation measures, even though I do not follow this approach here. See [Aït-Sahalia and Jacod \(2014\)](#) for a collection of both classical and more modern results on the asymptotic theory of these objects.

Table 3: Coefficient estimates from (22). Variables are always standardized before running the regression. Standard errors are computed using the HAC estimator from Newey and West (1987). Stars denote significance at 10%, 5%, and 1%, respectively. Different panels refer to different subsamples.

Panel A: Full Sample (January, 1973 - December, 2022)						
	BPV_1	BPV_2	BPV_3	$BPCov_{21}$	$BPCov_{31}$	$BPCov_{32}$
Average β_1	0.341*** (0.112)	0.561*** (0.175)	2.897*** (0.863)	-0.141** (0.065)	-0.562** (0.220)	0.136 (0.099)
Average β_2	0.340* (0.174)	0.874*** (0.318)	3.770*** (1.382)	-0.152 (0.106)	-0.639** (0.303)	0.038 (0.100)
Average β_3	-0.248** (0.116)	-0.537*** (0.206)	-1.679* (0.880)	0.194** (0.076)	0.253 (0.168)	0.028 (0.078)
N	600	600	600	600	600	600
R^2	0.18	0.31	0.27	0.08	0.18	0.02
Panel B: High Inflation and Volcker's Tenure (January, 1973 - August, 1987)						
	BPV_1	BPV_2	BPV_3	$BPCov_{21}$	$BPCov_{31}$	$BPCov_{32}$
Average β_1	0.901*** (0.161)	1.151*** (0.240)	5.065*** (1.433)	-0.438*** (0.106)	-1.230*** (0.424)	0.385 (0.242)
Average β_2	0.614*** (0.162)	1.377*** (0.274)	7.246*** (1.446)	-0.308*** (0.119)	-1.182*** (0.448)	0.252 (0.188)
Average β_3	0.094 (0.225)	-0.239 (0.358)	2.129 (1.654)	0.006 (0.178)	-0.616 (0.421)	0.655** (0.315)
N	176	176	176	176	176	176
R^2	0.40	0.47	0.40	0.20	0.30	0.07
Panel C: Post-Volcker Sample (September, 1987 - December, 2022)						
	BPV_1	BPV_2	BPV_3	$BPCov_{21}$	$BPCov_{31}$	$BPCov_{32}$
Average β_1	-0.026 (0.044)	-0.006 (0.051)	0.364 (0.296)	0.059 (0.038)	0.015 (0.055)	-0.044 (0.055)
Average β_2	-0.054 (0.069)	-0.026 (0.084)	-0.558 (0.516)	0.077 (0.060)	-0.037 (0.103)	0.001 (0.123)
Average β_3	-0.100 (0.082)	-0.145 (0.090)	-0.206 (0.517)	0.106 (0.071)	0.119 (0.105)	-0.069 (0.083)
N	424	424	424	424	424	424
R^2	0.07	0.08	0.06	0.13	0.02	0.01

Figure 5: Factor estimates associated to the first component of the panel generated by residuals from (21) and (22). The sample ranges from 1973 to 2022. Gray bars denote NBER recessions. The series is demeaned and scaled to have unit variance.



I also investigate the time-series evolution of this first principal component of these panels of residuals. Both time series are reported in Figure 5. The solid blue line represents the first principal component of the panel of residuals $\epsilon_{i,j}(t)$. The dashed orange line represents the first principal component from the panel of residuals $\eta_{i,j}(t)$. I also center both series at zero and make them have standard deviation equal to one before plotting them.

The two series are almost on top of each other, which tells us that the behavior of the first principal component of residuals is similar no matter whether we consider a pure-diffusion or a jump-diffusion setting. It typically spikes during recessions. Examples of that behavior happened in the early 1980s, during the dot-com bubble and the global financial crisis. We can spot a sharp spike during March, 2020. There are other sharp spike not related to recessions as well. For example, we can also see a spike during October, 1987 - exactly the month in which the “Black Monday” happened. Moreover, we can also see a sharp increase in late 2011, which coincides with the so-called “Operation Twist”, which was an attempt by the Federal Reserve to lower long-term yields by selling short-term Treasury securities and using the proceeds to buy long-term obligations.¹⁸ Additionally, this time series is skewed in the sense that its largest realizations are all on the positive plane. It doesn’t have large spikes down - as one would expect once in a while if it were pure noise.

In contrast, Figure A.5 in Appendix A displays the second principal component of the panel of errors. The behavior is entirely different. The solid and the dashed line are not tracking each other so well and there are spikes in both directions. The behavior during recessions does not have a clear pattern. These time series are more consistent with pure noise. Figure A.6, also in Appendix A, displays the autocorrelation functions for both the first and second principal components. While the first principal component is a persistent time series with autocorrelations that are positive and decay slowly, the second principal component has autocorrelations that are often not significant and that are typically small in absolute value. Taken together, the evidence from this section leads us to conclude that there is unspanned volatility across the entire yield curve and the residual variation that cannot be explained by the cross-section of yields has a strong one-factor structure.

¹⁸See [Blinder \(2022\)](#) and [Bernanke \(2023\)](#) for a discussion about Operation Twist and other unconventional measures taken during this time.

6 How Jumpy Are the Nelson-Siegel Factors?

We now study the variation in the Nelson-Siegel factors that comes from jumps. The variation that comes from jumps can be estimated in the following way:

$$JV_i(t) \equiv \max\{RCov_{ii}(t) - BPV_i(t), 0\}, \quad i = 1, 2, 3 \quad (23)$$

In finite samples, it can be the case that $RCov_{ii}(t) - BPV_i(t) < 0$, even though that won't happen in the limit. [Barndorff-Nielsen and Shephard \(2004\)](#) show, with simulation evidence, that this estimator performs well in a variety of scenarios. Figure 6 displays the time-series evolution of the square root of the jump variation (so it's on a similar scale to Figure 2). It also spikes up during the high inflation era during the 1970s and during the initial phase of Volcker's tenure. The 2008 crisis also represents another moment where the jump variation gets more active.

It's also convenient to consider the ratio between realized variance and jump variation. This ratio represents how much of the total variation in each of the Nelson-Siegel factors is due to jumps:¹⁹

$$JR_i(t) \equiv \frac{JV_i(t)}{RCov_{ii}(t)}, \quad i = 1, 2, 3 \quad (24)$$

[Huang and Tauchen \(2005\)](#) analyzed how big the term in (24) is for the case of equities in the US. They found an average jump ratio of about 7%. Table 4 displays the average jump ratio over the entire sample for each factor. They surprisingly close to each other, but double the size of the mean jump ratio for the equities. Although the Nelson-Siegel factors capture movements that very different across maturities, they all seem to have the same average "jumpiness".

6.1 FOMC Announcements

Given the evidence in [Andersen et al. \(2007\)](#), it's natural to ask whether macroeconomic announcements, such as the ones from the Federal Open Market Committee (FOMC) are related to the jumpiness of Nelson-Siegel factors. I analyze here how volatility of factors, the jumpiness, and unspanned volatility vary with monetary policy shocks. To do that, I rely on a dataset the dataset from [Swanson \(2021\)](#) who used intraday futures data to extract surprises around FOMC announcements in the Eurodollar and Fed Funds market.

The dataset provides three time-series of shocks. The first one is a Fed Funds rate shock, a standard monetary policy shock (FFR). The second one is a "forward guidance" shock (FG), which does not move the very short rates by construction but is designed to capture shocks to yields a few months ahead. The third shock is related to large-scale asset purchases (LSAP) - or Quantitative Easing. It affects yields with maturities with more than five years. They are plotted in Figure A.7 in Appendix A. Positive values imply a monetary tightening. The dataset ranges from January 1991 to June, 2019.²⁰

¹⁹I only define this measure for realized variance and ignore covariances because the covariances might be negative or even zero. In that case, the notion of a jump ratio is not well defined.

²⁰I only plot LSAP from 2008 onwards since that will be the relevant period for regressions when it's used. Although there were no LSAPs prior to 2008, the shock identification technique used to extract this delivers a time series with the same length for all of them. But realizations of LSAP prior to 2008 in Eric Swanson's dataset are, by construction, minuscule. See [Swanson \(2021\)](#) for further details.

Figure 6: Square root of jump variation for each factor, as defined in (23). The sample ranges from 1973 to 2022. Gray bars denote NBER recessions. The scale is the same as the one from Figure 2.

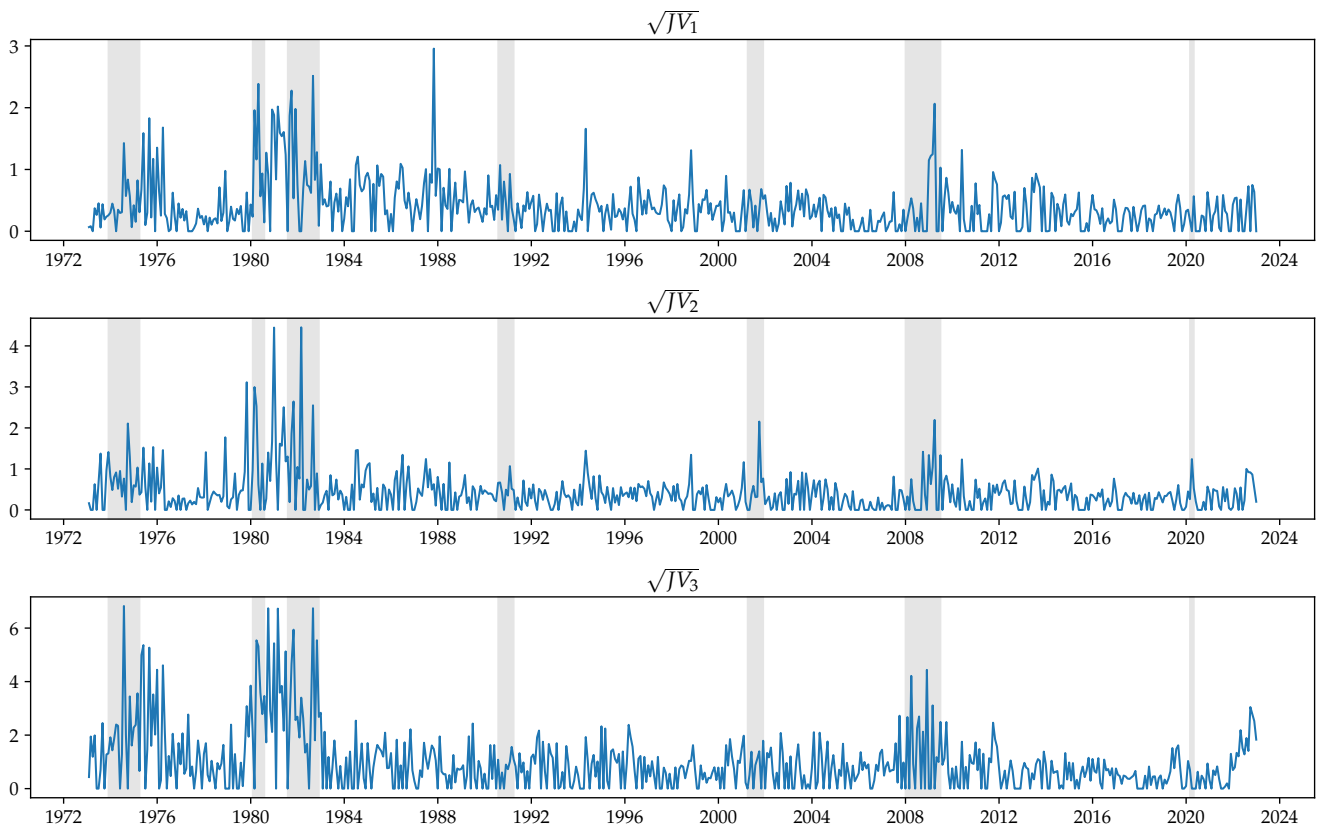


Table 4: The first two panels show the average for each variable conditional on the existence of an FOMC announcement, following the dates from Swanson (2021). The p -value refers to a test whether both averages are the same. A low p -value indicates that average are statistically different. The last panel displays the average jump volatility ratio for the whole sample and conditional on FOMC announcements following the dates in Swanson (2021).

Panel A: Average Realized Covariation						
	$RCov_{11}$	$RCov_{22}$	$RCov_{33}$	$RCov_{21}$	$RCov_{31}$	$RCov_{32}$
No FOMC Meeting	0.999	1.215	6.016	-0.969	-0.137	-0.214
FOMC Meeting	1.219	1.520	6.797	-1.123	-0.371	-0.168
p -value	0.001	0.025	0.058	0.029	0.027	0.765
Panel B: Average Realized Bipower Covariation						
	BPV_1	BPV_2	BPV_3	$BPCov_{21}$	$BCov_{31}$	$BCov_{32}$
No FOMC Meeting	0.876	1.048	5.107	-0.867	-0.145	-0.125
FOMC Meeting	1.049	1.325	5.984	-0.980	-0.422	-0.145
p -value	0.016	0.014	0.081	0.150	0.019	0.905
Panel C: Average Jump Variation Fraction						
	JR_1	JR_2	JR_3			
Whole Sample (1973-2022)	0.172	0.158	0.170			
No FOMC Meeting	0.146	0.145	0.161			
FOMC Meeting	0.150	0.149	0.157			
p -value	0.799	0.808	0.812			

Table 4 reports the average realized covariance and realized bipower covariation measures over months with and without FOMC announcements, taken from Swanson’s dataset. For each column, the p -value reported is associated to a test of null of equal (co)-variation. As expected, once more validating the variation measures, there is more overall volatility on months with FOMC announcements. There is also more diffusive volatility across the board. The behavior of the cross-terms is mixed.

Alternatively, the jumpiness of the Nelson-Siegel factors remains constant no matter an FOMC announcement happened or not. This is evidence that, even though overall volatility increases, the amount of volatility due to jumps remains constant over time - around 15%. To the best of my knowledge, this is the first study to document such stable behavior.

6.2 Monetary Policy Surprises and Volatility

Following the insight from Kuttner (2001), if market participants are not surprised during a monetary policy announcement, there should be no specific asset price movements. In that spirit, instead of conditioning on the existence of a monetary policy announcement, I now consider the projection of different variables on absolute values of these surprises. I consider regressions of the following form

$$Z_t = \alpha + \theta \times |\text{Shock}|_t + u_t \quad (25)$$

Table 5: Coefficient estimates from (25) when the realized bipower variation for each one of the factors is used as the dependent variable. The first three columns refer to the 1991-2019 period, while the fourth column for each dependent variables concentrates on the zero-lower bound period. Variables are standardized before running the regression. Stars denote significance at 10%, 5%, and 1%, respectively.

	BPV_1				BPV_2				BPV_3			
	(1)	(2)	(3)	(4)	(5)	(6)	(7)	(8)	(9)	(10)	(11)	(12)
FFR	0.20** (0.10)		0.15* (0.09)		0.35*** (0.12)		0.32** (0.13)		0.26** (0.10)		0.22** (0.10)	
FG		0.20*** (0.08)	0.15** (0.07)	0.22 (0.16)		0.18*** (0.06)	0.07 (0.05)	0.14 (0.11)		0.18*** (0.06)	0.10* (0.06)	0.26* (0.14)
LSAP				0.03 (0.09)				0.05 (0.07)				-0.02 (0.09)
N	336	336	336	109	336	336	336	109	336	336	336	109
R ²	0.04	0.04	0.06	0.06	0.12	0.03	0.12	0.03	0.07	0.03	0.08	0.06

where Z_t is a generic variable of interest. Before running the regression, I scale the variables so a shock of one standard deviation (no matter the sign) changes Z_t by θ standard deviations, on average.

Table 5 displays results the results when we project the realized bipower variation measures into the absolute value of monetary policy surprises.²¹ For each dependent variable, the first and second columns analyze the effect of FFR and FG shocks individually. The third one conditions on both of them. Finally, the fourth sample considers the period of the Zero Lower Bound, when there was no FFR shock by design and both Quantitative Easing and forward guidance were used together.²²

Across the board, a shock in the Federal Funds rate does increase the diffusive volatility of Nelson-Siegel factors. This is intuitive since, after a shock, agents might still take time to learn the fundamental reason why they were surprised and then update their trading positions, generating higher volatility over the rest of the month. When conditioning on both FFR and FG, both are still significant with the exception of BVP_2 . We don't find evidence, however, that LSAPs increased the diffusive volatility.

Table 6 repeats this analysis but now focusing on JR_i . Consistent with the previous evidence, most of the coefficients are not statistically different than zero. The only exception at the 5% level would be the coefficient on LSAP for JR_1 . But in general it's hard to make the case that monetary policy surprises are making the yield curve relatively "more jumpy". Unreported results show that JV does increase with monetary policy announcements, but argue that it increases in a proportional way to the diffusive volatility. This is consistent with a setting in which agents process information, and update their positions, as new information gets released on, for example, a daily basis. Even though FOMC announcements move markets on the day they happen, the period before and the period after the announcement is also more volatile.

²¹I focus here only variances and not on covariances because they are quantitatively less important. Results are available upon request, however.

²²I refer to Kuttner (2018) for an assessment of unconventional monetary policy over time.

Table 6: Coefficient estimates from (25) when the realized jump variation ratio for each one of the factors, as in (24), is used as the dependent variable. The first three columns refer to the 1991-2019 period, while the fourth column for each dependent variables concentrates on the zero-lower bound period. Variables are standardized before running the regression. Stars denote significance at 10%, 5%, and 1%, respectively.

	JR_1				JR_2				JR_3			
	(1)	(2)	(3)	(4)	(5)	(6)	(7)	(8)	(9)	(10)	(11)	(12)
FFR	0.07 (0.06)		0.07 (0.07)		0.03 (0.04)		0.03 (0.05)		0.06 (0.07)		0.03 (0.07)	
FG		0.02 (0.05)	-0.00 (0.05)	0.00 (0.10)		0.02 (0.06)	0.01 (0.07)	0.13 (0.10)		0.08* (0.05)	0.07 (0.05)	0.09 (0.11)
LSAP				0.20** (0.10)				0.18 (0.13)				-0.11* (0.06)
N	336	336	336	109	336	336	336	109	336	336	336	109
R^2	0.00	0.00	0.00	0.04	0.00	0.00	0.00	0.07	0.00	0.01	0.01	0.01

7 How Much of Unspanned Volatility Is Due to Monetary Policy Shocks?

In this last analysis, we revisit the evidence from Section 5 and ask whether these monetary policy surprises can account for unspanned volatility. If these time series are indeed pure shocks, they should not be spanned by the cross-section of yields. After all, in the standard affine term-structure models there is typically no role for a central bank aside from a simple policy rule like (3). Therefore, after a shock, agents can update their positions based on new information and generate volatility that could not possibly be spanned by the yield curve. The empirical question is how of that variation can be accounted by monetary policy. Importantly, *ex-ante*, it's not clear whether different instruments of monetary policy generate volatility in the same way.

In this spirit, Table 7 reports coefficients for the projection of the first principal component of the residuals $\eta_{i,j}(t)$, which corresponds to the dashed line in Figure 5, on the monetary policy shocks. Once more, both the dependent and the independent variables are standardized before the running the regression. The answer for the question in the title of this section is “not much”. The values for R^2 reported in Table 7 are never past 0.08. But I do find a significant effect of forward guidance shocks on the first principal component of residuals. On the contrary, I find no evidence that a standard Fed Funds shock increased the amount of unspanned volatility.

The last fours columns of Table 7 repeat the analysis for the second principal component of residuals. In line with the previous interpretation that the second principal component encodes no relevant information and is mostly just noise, I find essentially no significant coefficients.

In order to check the robustness of these results, I regress the residuals $\eta_{i,j}(t)$ individually on the monetary policy surprises. Results are reported in Table 8. Consistent with the interpretation that forward guidance shocks fuel unspanned volatility, I find that coefficients on FG are positive and statistically significant across specifications. Coefficients on other shocks are not significant, usually. The values for R^2 are still low, nonetheless.

In summary, I provide evidence in this section that forward guidance shocks indeed fuel the unspanned part of yield curve volatility. However, these shocks can only explain a small part of the time series evolution of yield

Table 7: Coefficient estimates from (25) when the principal components of $\eta_{i,j}(t)$ are used as the dependent variables. The first three columns refer to the 1991-2019 period, while the fourth column for each dependent variables concentrates on the zero-lower bound period. Variables are standardized before running the regression. Stars denote significance at 10%, 5%, and 1%, respectively.

	First PC of Residuals				Second PC of Residuals			
	(1)	(2)	(3)	(4)	(5)	(6)	(7)	(8)
FFR	0.10 (0.10)		0.04 (0.09)		0.16* (0.09)		0.15 (0.09)	
FG		0.17** (0.08)	0.16** (0.07)	0.30* (0.17)		0.09 (0.07)	0.04 (0.07)	-0.03 (0.18)
LSAP				-0.05 (0.09)				0.02 (0.07)
N	336	336	336	109	336	336	336	109
R^2	0.01	0.03	0.03	0.08	0.03	0.01	0.03	0.00

volatility above and beyond what is already spanned by bond prices. This is true even when we consider the presence of jumps to extract the dynamics of unspanned volatility.

8 Conclusion

As [Duffee \(2002\)](#) points out, affine term-structure models face a trade-off between fitting the cross-section of yields and fitting their time-series behavior. In this paper, I consider implications for the volatilities of yields that arise naturally in the context of these models. I extended results from [Andersen and Benzoni \(2010\)](#) to general linear combinations of yields in a jump-diffusion. I also proposed a new way to test for the presence of unspanned volatility based jump-robust estimators of the diffusive variance of Nelson-Siegel factors. My approach does not rely on any assumptions about the empirical relevance of the drift in yields and I do not constrain the dynamics of the underlying risk factors under the physical measure.

The results point to a stark inability of affine term structure models to accommodate the volatility behavior we see from yields. The part of volatility that cannot be spanned by yields has a strong 1-factor structure. This finding is robust across subsamples that exclude the exceptional years of the great inflation from 1970s and subsequent monetary tightening. I also test whether monetary policy shocks can explain unspanned volatility. I do find that forward-guidance-type shocks fuel volatility in yields, across the entire yield curve. However, such shocks explain less than 10% of unspanned volatility.

Understanding the sources of variation in yields is a prime concern for risk managers and traders seeking to hedge fixed income portfolios. Although it might contain a purely stochastic nature to some extent, movements in asset prices - which generates volatility more generally - should be tied to economic fundamentals. Explaining the “excessive variation” I document here with macroeconomic and financial indicators seems a natural next step into understanding

Table 8: Coefficient estimates from (25) using the residuals directly as dependent variables. The first three columns refer to the 1991-2019 period, while the fourth column for each dependent variables concentrates on the zero-lower bound period. Variables are standardized before running the regression. Stars denote significance at 10%, 5%, and 1%, respectively.

	$\eta_{11}(t)$				$\eta_{22}(t)$				$\eta_{33}(t)$			
	(1)	(2)	(3)	(4)	(5)	(6)	(7)	(8)	(9)	(10)	(11)	(12)
FFR	0.10 (0.10)		0.04 (0.08)		0.19* (0.10)		0.16 (0.11)		0.10 (0.09)		0.06 (0.08)	
FG		0.18** (0.08)	0.17** (0.07)	0.26* (0.15)		0.15*** (0.05)	0.10* (0.06)	0.19** (0.09)		0.15*** (0.06)	0.13** (0.06)	0.31** (0.14)
LSAP				-0.01 (0.09)				-0.03 (0.05)				-0.09 (0.08)
N	336	336	336	109	336	336	336	109	336	336	336	109
R ²	0.01	0.03	0.03	0.07	0.04	0.02	0.05	0.03	0.01	0.02	0.03	0.08

References

- Andersen, T. G. and Benzoni, L. (2008). Realized volatility. Working Paper Series WP-08-14, Federal Reserve Bank of Chicago.
- Andersen, T. G. and Benzoni, L. (2010). Do bonds span volatility risk in the u.s. treasury market? a specification test for affine term structure models. *The Journal of Finance*, 65(2):603–653.
- Andersen, T. G., Bollerslev, T., Diebold, F. X., and Vega, C. (2007). Real-time price discovery in global stock, bond and foreign exchange markets. *Journal of International Economics*, 73(2):251–277.
- Ang, A. and Piazzesi, M. (2003). A no-arbitrage vector autoregression of term structure dynamics with macroeconomic and latent variables. *Journal of Monetary Economics*, 50(4):745–787.
- Aït-Sahalia, Y. and Jacod, J. (2014). *High-Frequency Financial Econometrics*. Princeton University Press.
- Barndorff-Nielsen, O. and Shephard, N. (2004). Power and bipower variation with stochastic volatility and jumps. *Journal of Financial Econometrics*, 2(1):1–37.
- Barndorff-Nielsen, O. and Shephard, N. (2006). Econometrics of testing for jumps in financial economics using bipower variation. *Journal of Financial Econometrics*, 4(1):1–30.
- Bauer, M. D. and Hamilton, J. D. (2018). Robust bond risk premia. *Review of Financial Studies*, 31(2):399–448.
- Bauer, M. D. and Rudebusch, G. D. (2020). Interest Rates under Falling Stars. *American Economic Review*, 110(5):1316–1354.
- Bernanke, B. (2023). *21st Century monetary policy: The Federal Reserve from the great inflation to COVID-19*. W. W. Norton and Company.
- Bianchi, D., Büchner, M., and Tamoni, A. (2021). Bond risk premiums with machine learning. *Review of Financial Studies*, 34(2):1046–1089.
- Blinder, A. S. (2022). *Monetary and fiscal history of the United States, 1961-2021*. Princeton University Press.
- Cieslak, A. and Povala, P. (2015). Expected returns in treasury bonds. *Review of Financial Studies*, 28(10):2859–2901.
- Cochrane, J. H. and Piazzesi, M. (2005). Bond Risk Premia. *American Economic Review*, 95(1):138–160.
- Cooper, I. and Priestley, R. (2009). Time-varying risk premiums and the output gap. *Review of Financial Studies*, 22(7):2601–2633.
- Diebold, F. X. and Li, C. (2006). Forecasting the term structure of government bond yields. *Journal of Econometrics*, 130(2):337–364.
- Diebold, F. X. and Rudebusch, G. D. (2013). *Yield curve modeling and forecasting: the dynamic Nelson-Siegel approach*. The Econometric and Tinbergen Institutes lectures. Princeton University Press, Princeton.
- Diebold, F. X., Rudebusch, G. D., and Aruoba, S. B. (2006). The macroeconomy and the yield curve: a dynamic latent factor approach. *Journal of Econometrics*, 131(1-2):309–338.

- Duarte, J. (2004). Evaluating an alternative risk preference in affine term structure models. *Review of Financial Studies*, 17(2):379–404.
- Duffee, G. (2002). Term premia and interest rate forecasts in affine models. *Journal of Finance*, 57(1):405–443.
- Duffee, G. (2013a). Forecasting interest rates. In *Handbook of Economic Forecasting*, pages 385–426. Elsevier.
- Duffee, G. R. (2013b). Bond pricing and the macroeconomy. In *Handbook of the Economics of Finance*, pages 907–967. Elsevier.
- Duffie, D. and Kan, R. (1996). A yield-factor model of interest rates. *Mathematical Finance*, 6(4):379–406.
- Duffie, D., Pan, J., and Singleton, K. (2000). Transform analysis and asset pricing for affine jump-diffusions. *Econometrica*, 68(6):1343–1376.
- Fama, E. and Bliss, R. R. (1987). The information in long-maturity forward rates. *American Economic Review*, 77(4):680–92.
- Fernandes, M. and Vieira, F. (2019). A dynamic nelson–siegel model with forward-looking macroeconomic factors for the yield curve in the US. *Journal of Economic Dynamics and Control*, 106:103720.
- Freire, G. and Riva, R. (2023). Asymmetric violations of the spanning hypothesis. *SSRN Electronic Journal*.
- Gurkaynak, R. S., Sack, B., and Wright, J. H. (2007). The U.S. Treasury yield curve: 1961 to the present. *Journal of Monetary Economics*, 54(8):2291–2304.
- Gürkaynak, R., Sack, B., and Swanson, E. (2005). Do actions speak louder than words? the response of asset prices to monetary policy actions and statements. *International Journal of Central Banking*, 1(1).
- Huang, X. and Tauchen, G. (2005). The relative contribution of jumps to total price variance. *Journal of Financial Econometrics*, 3(4):456–499.
- Hännikäinen, J. (2017). When does the yield curve contain predictive power? evidence from a data-rich environment. *International Journal of Forecasting*, 33(4):1044–1064.
- Joslin, S., Pribsch, M., and Singleton, K. (2014). Risk premiums in dynamic term structure models with unspanned macro risks. *Journal of Finance*, 69(3):1197–1233.
- Kuttner, K. N. (2001). Monetary policy surprises and interest rates: Evidence from the fed funds futures market. *Journal of Monetary Economics*, 47(3):523–544.
- Kuttner, K. N. (2018). Outside the box: Unconventional monetary policy in the great recession and beyond. *Journal of Economic Perspectives*, 32(4):121–146.
- Litterman, R. B. and Scheinkman, J. (1991). Common factors affecting bond returns. *Journal of Fixed Income*, 1(1):54–61.
- Liu, Y. and Wu, C. (2021). Reconstructing the yield curve. *Journal of Financial Economics*, 142(3):1395–1425.
- Ludvigson, S. and Ng, S. (2009). Macro factors in bond risk premia. *Review of Financial Studies*, 22(12):5027–5067.
- Nelson, C. and Siegel, A. F. (1987). Parsimonious modeling of yield curves. *Journal of Business*, 60(4):473–89.

- Newey, W. K. and West, K. D. (1987). A Simple, Positive Semi-definite, Heteroskedasticity and Autocorrelation Consistent Covariance Matrix. *Econometrica*, 55(3):703–708.
- Piazzesi, M. (2005). Bond yields and the federal reserve. *Journal of Political Economy*, 113(2):311–344.
- Piazzesi, M. (2010). *Affine Term Structure Models*, page 691–766. Elsevier.
- Svensson, L. E. O. (1994). Estimating and interpreting forward interest rates: Sweden 1992-1994. *IMF Working Papers*, 94(114):1.
- Swanson, E. T. (2021). Measuring the effects of federal reserve forward guidance and asset purchases on financial markets. *Journal of Monetary Economics*, 118:32–53.

Supplementary Appendix

A Figures

Figure A.1

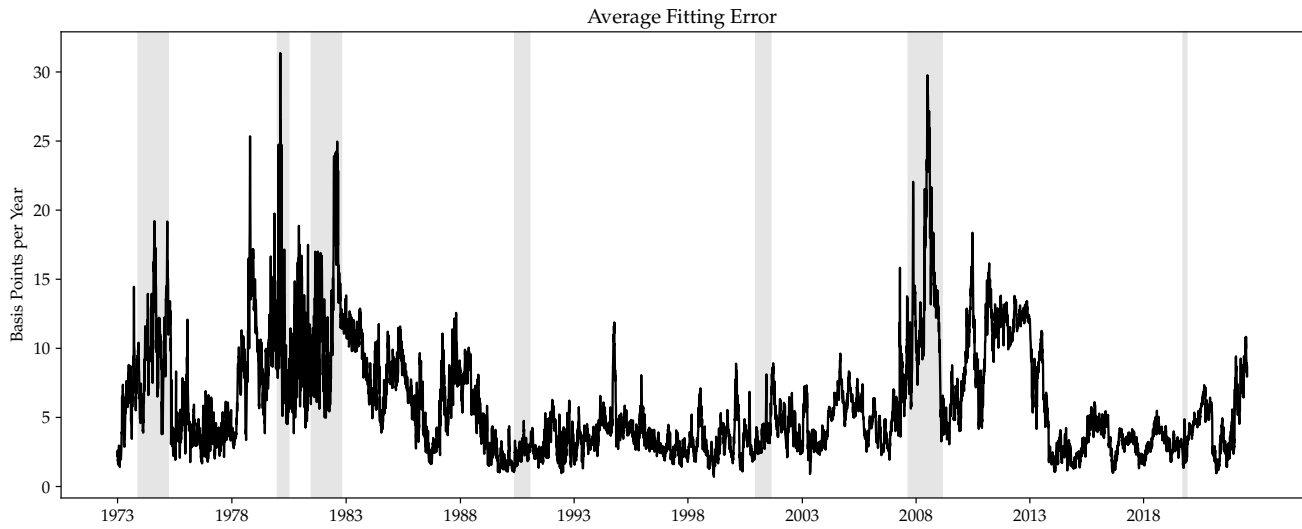


Figure A.2

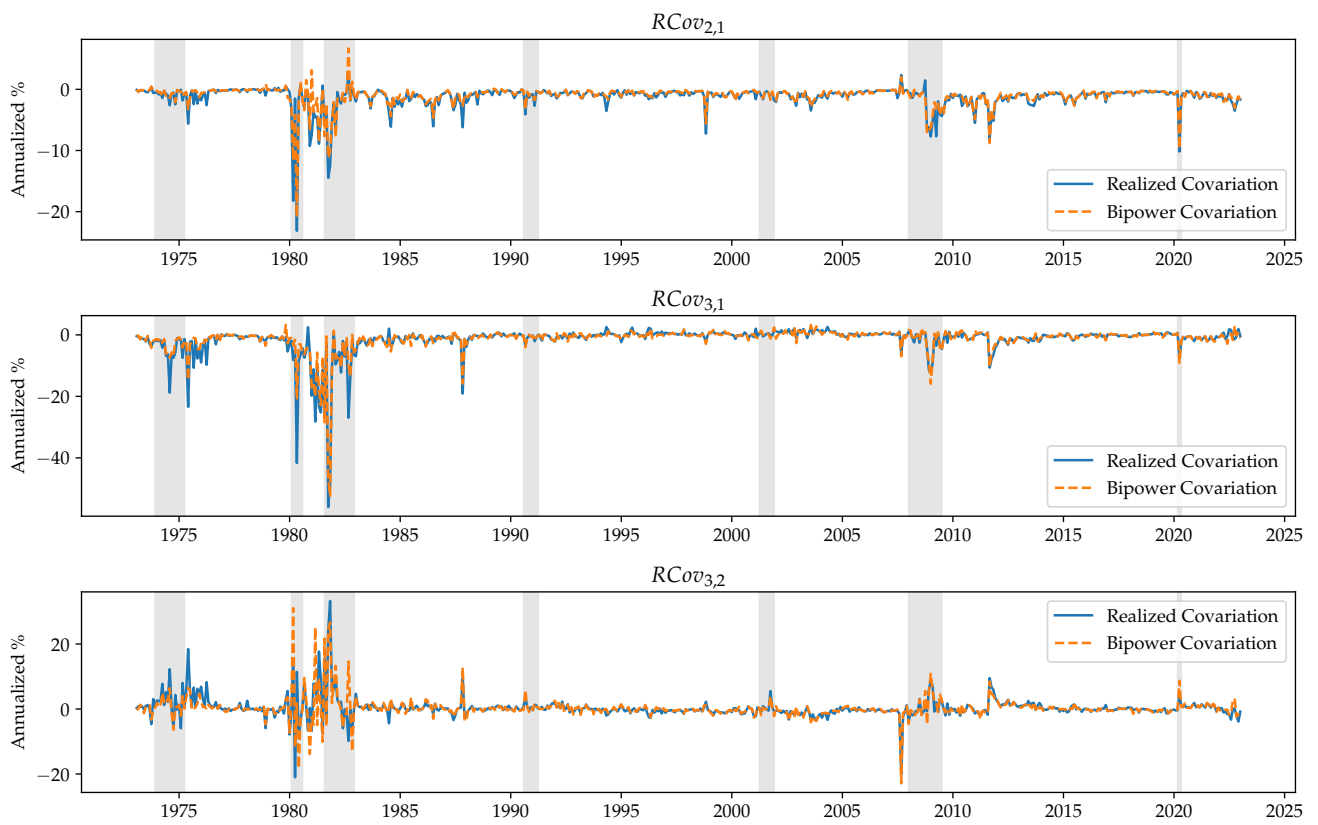


Figure A.3

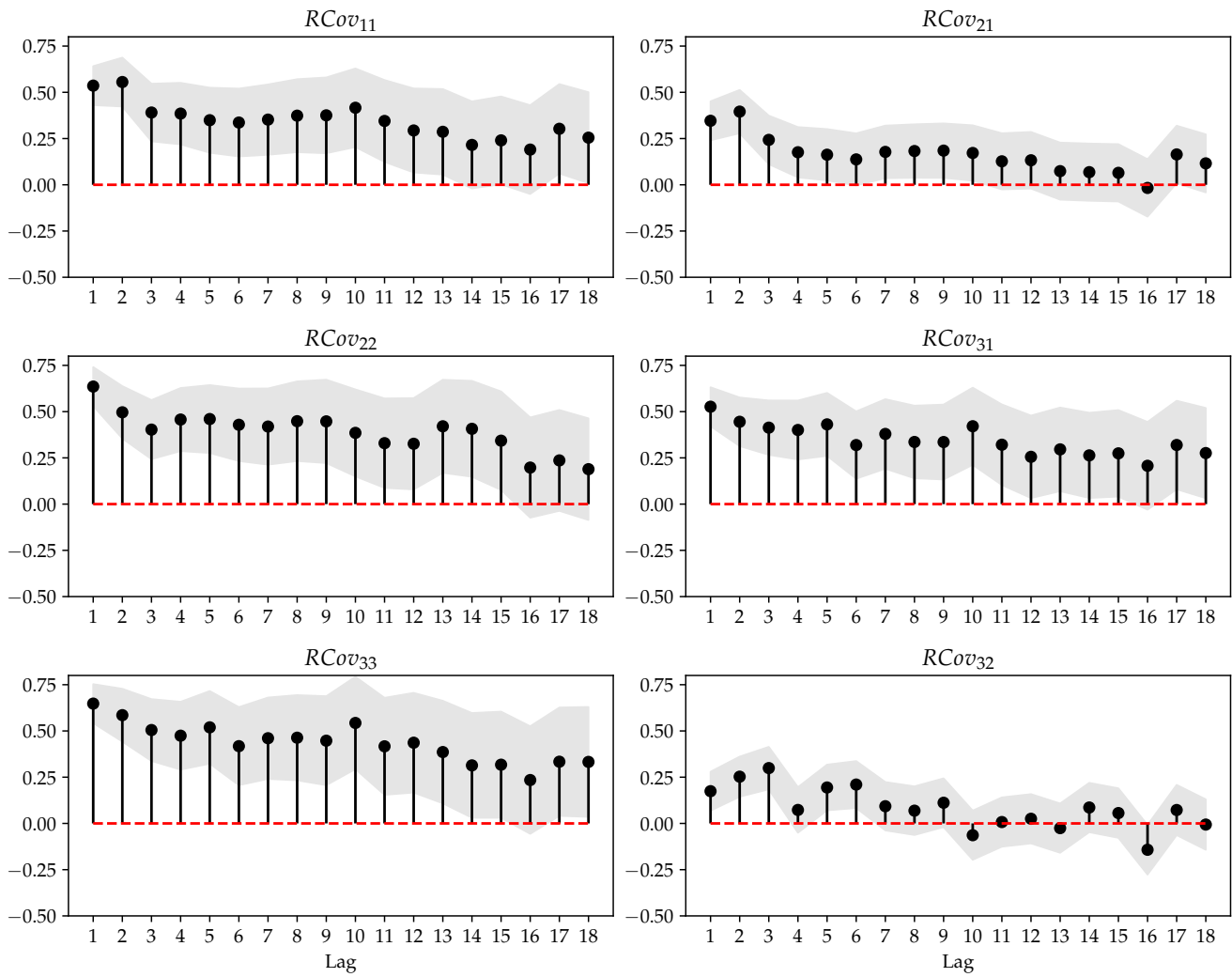


Figure A.4

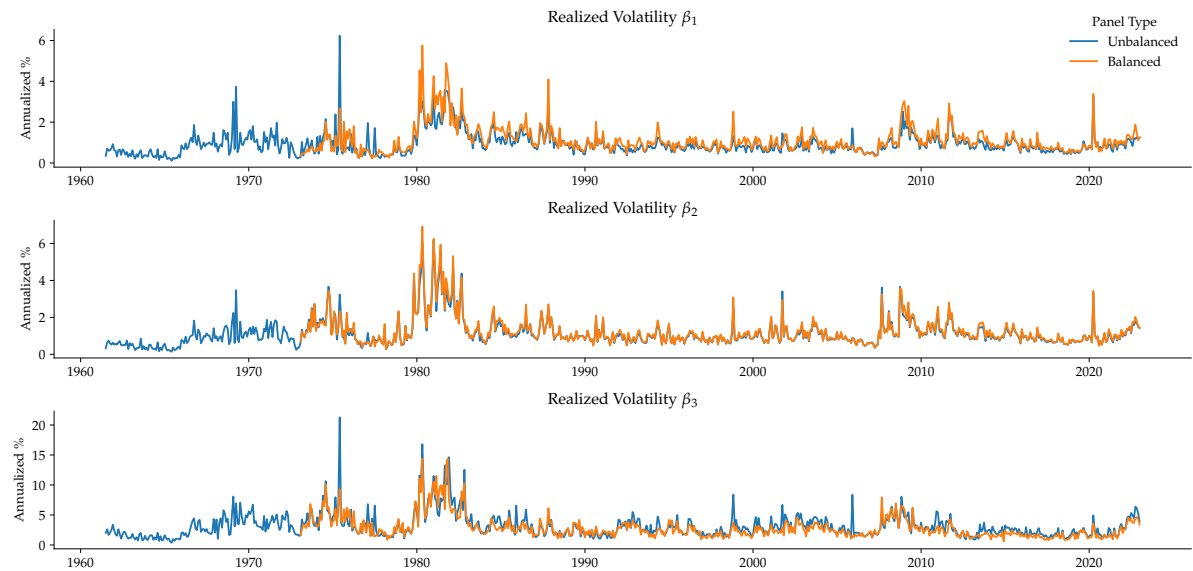


Figure A.5

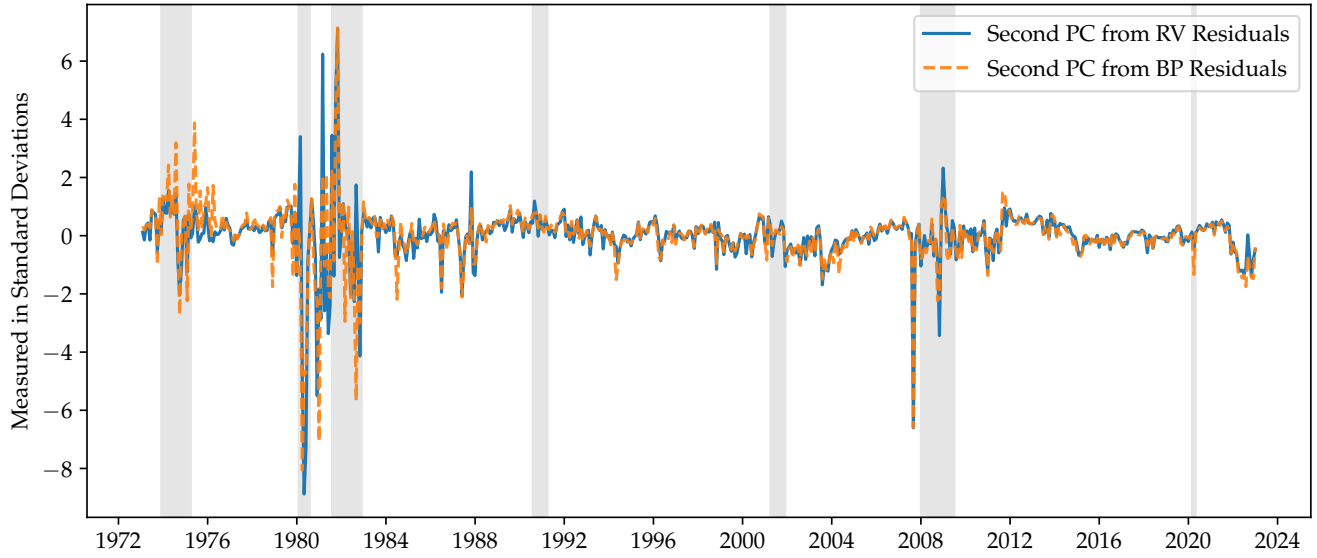
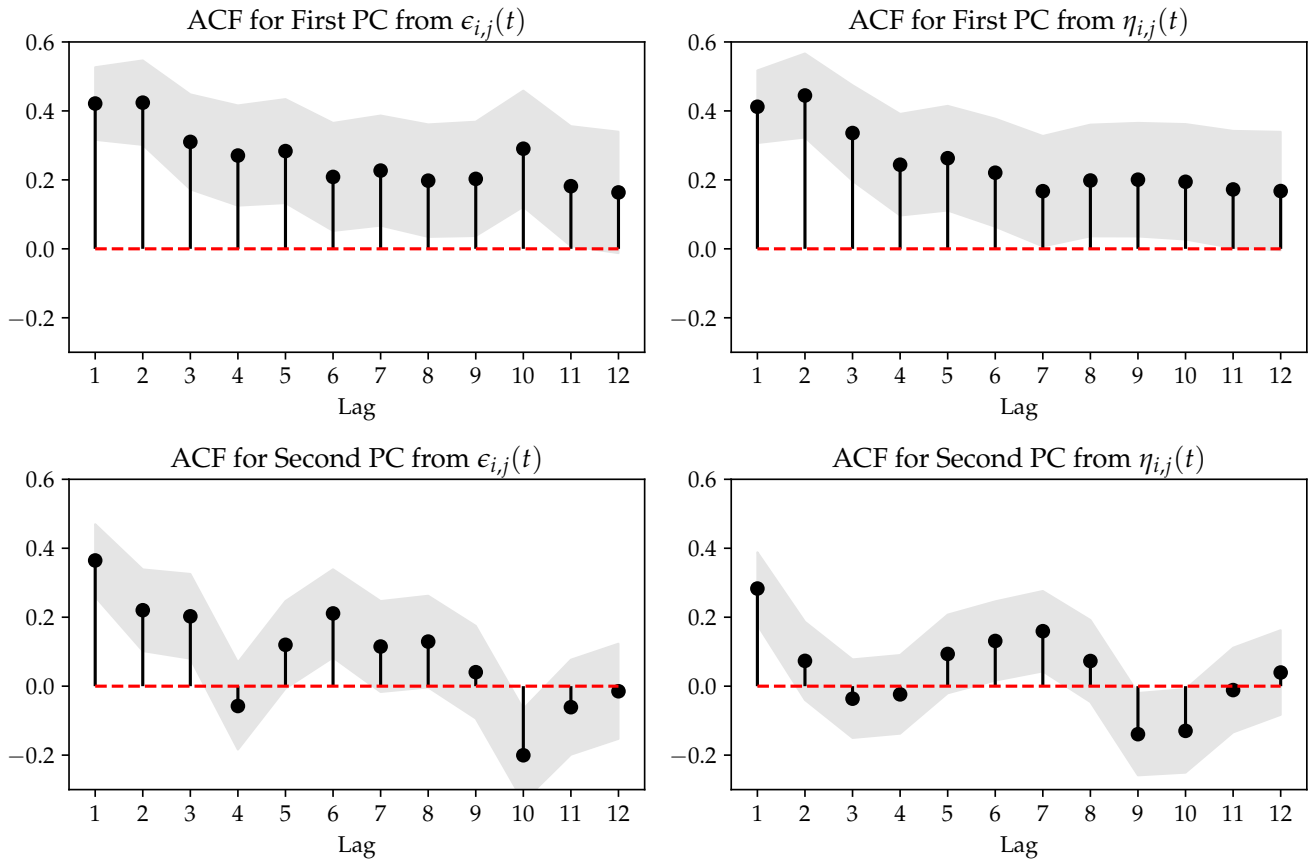


Figure A.6



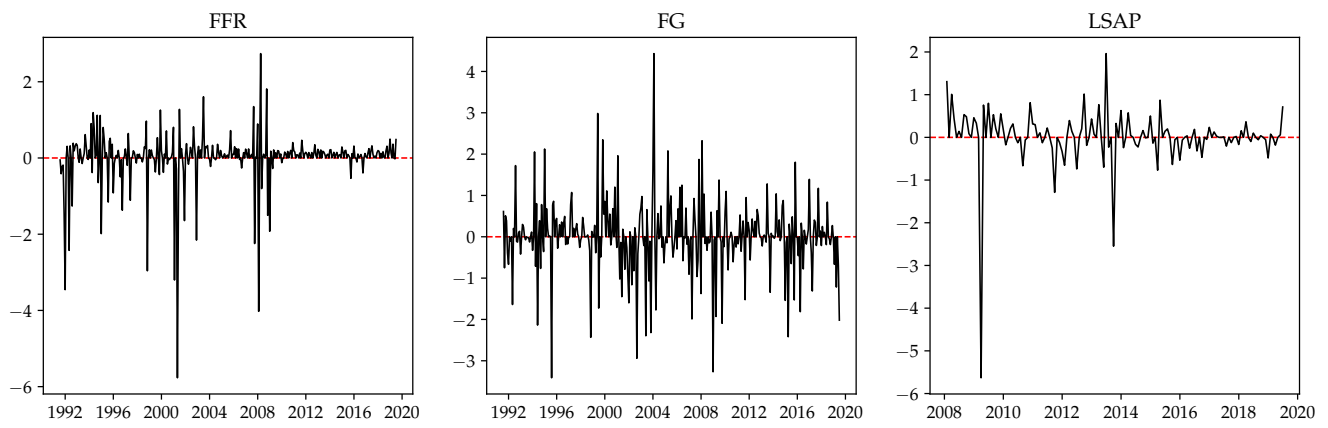


Figure A.7

B Tables

Table B.1: Robustness check. See Table 2.

	$RCov_{11}$	$RCov_{22}$	$RCov_{33}$	$RCov_{21}$	$RCov_{31}$	$RCov_{32}$
PC1	1.013*** (0.353)	1.632*** (0.484)	9.337*** (2.671)	-0.302 (0.208)	-1.896*** (0.699)	0.489 (0.393)
PC2	0.145 (0.251)	0.894** (0.418)	3.600* (1.839)	-0.010 (0.159)	-0.670* (0.378)	0.057 (0.178)
PC3	0.721** (0.344)	1.586*** (0.585)	4.699* (2.588)	-0.494** (0.213)	-0.871* (0.512)	0.157 (0.232)
PC4	0.462* (0.259)	0.187 (0.439)	0.801 (1.884)	-0.212 (0.147)	-0.274 (0.474)	-0.218 (0.252)
PC5	0.004 (0.190)	0.039 (0.313)	1.141 (1.519)	-0.037 (0.121)	-0.393 (0.352)	0.158 (0.151)
PC6	-0.063 (0.241)	-0.301 (0.316)	-2.666 (1.864)	-0.053 (0.169)	0.157 (0.451)	0.118 (0.285)
N	600	600	600	600	600	600
R2	0.22	0.33	0.29	0.10	0.21	0.03

Table B.2: Robustness check. See Table 3.

	BPV_1	BPV_2	BPV_3	$BPCov_{21}$	$BPCov_{31}$	$BPCov_{32}$
PC1	0.755** (0.293)	1.223*** (0.391)	7.608*** (2.186)	-0.172 (0.180)	-1.537** (0.641)	0.448 (0.337)
PC2	0.131 (0.199)	0.678** (0.332)	3.037** (1.490)	-0.002 (0.126)	-0.483 (0.325)	-0.021 (0.136)
PC3	0.642** (0.272)	1.324*** (0.489)	4.658** (2.074)	-0.442*** (0.166)	-0.761* (0.411)	0.005 (0.156)
PC4	0.406* (0.208)	0.139 (0.346)	0.535 (1.418)	-0.228* (0.137)	-0.142 (0.370)	0.228 (0.229)
PC5	0.015 (0.157)	0.078 (0.245)	0.606 (1.182)	-0.035 (0.108)	-0.201 (0.268)	0.166 (0.125)
PC6	-0.063 (0.193)	-0.175 (0.267)	-2.055 (1.421)	-0.076 (0.143)	0.137 (0.367)	0.010 (0.266)
N	600	600	600	600	600	600
R2	0.22	0.31	0.28	0.10	0.19	0.02